DMRT5, DMRT3 and EMX2 cooperatively repress *Gsx2* at the pallium-subpallium boundary tomaintain cortical identity in dorsal telencephalic progenitors

Elodie Desmaris1, Marc Keruzore1,†, Amandine Saulnier1,†, Leslie Ratié1, Stavroula Assimacopoulos2, Sarah De Clercq1, Xinsheng Nan3, Kaushik Roychoudhury4, Shenyue Qin4, Sadia Kricha1, Clément Chevalier5, Thomas Lingner6, Kristine A. Henningfeld7, David Zarkower8, Antonello Mallamaci9, Thomas Theil10, Kenneth Campbell4, Tomas Pieler7, Meng Li3, Elizabeth A. Grove2,*, Eric J. Bellefroid1,*

1 Université Libre de Bruxelles (ULB), ULB Institute of Neuroscience (UNI), B-6041 Gosselies, Belgium;

2 Department of Neurobiology, University of Chicago, Chicago, Illinois 60637, USA;

3 Neuroscience and Mental Health Research Institute, School of Medicine and School of Biosciences, Cardiff University, Cardiff, CF24 4HQ, UK;

4 Division of Developmental Biology, Cincinnati Children's Hospital Medical Center, University of Cincinnati College of Medicine, Cincinnati, OH 45229, USA;

5 Center for Microscopy and Molecular Imaging, B-6041 Gosselies, Belgium;

6 Microarray and Deep-Sequencing Core facility, University Medical Center Göttingen (UMG), Justus-von-Liebig-Weg 11, 37077 Göttingen, Germany;

7 Department of Developmental Biochemistry, Center for Nanoscale Microscopy and Molecular Physiology of the Brain (CNMPB), University of Göttingen, 37077 Göttingen, Germany;

8 Department of Genetics, Cell Biology and Development, University of Minnesota, Minneapolis, Minnesota 55455, USA;

9 Laboratory of Cerebral Cortex Development, SISSA, Trieste, Italy;

10 Centre for Integrative Physiology, University of Edinburgh, Edinburgh EH8 9XD, UK.

†These authors contributed equally to this work.

Co-corresponding authors: ebellefr@ulb.ac.be and egrove@bsd.uchicago.edu

ACKNOWLEDGEMENTS:
We thank Dr. D. Kawaguchi for kind gift of the *Foxg1-IRES-Cre* line used in this study; Dr. F. Guillemot, J. Rubenstein, S. Sahara, D. O'Leary, A. Chotteau-Lelièvre and Y. Sun for gifts of plasmid DNA, C. Parras for the Ascl1 antibody and L. Delhaye for technical help. This work was supported by grants from the FNRS (FRFC 6973823 and CDR 29148846) and the Walloon Region (First International project "CORTEX") and the Fonds pour la Recherche Médicale dans le Hainaut (FMRH). Work in the laboratories of EG, DZ and KC was supported by NIH grant RO1 MH103211, GM059152 and R01 NS044080, respectively. Work in the laboratory of TT was supported by grant BB/P00122X/1. Work in the Center for Microscopy

and Molecular Imaging was supported by the Hainaut-Biomed FEDER program. E.D is a Wallonie-Bruxelles International (WBI) doctoral fellow from the Wallonia-Brussels Federation. M.K was a First International and L.R a BEWARE postdoctoral fellow from the Walloon Region; S.D.C. was a FNRS postdoctoral fellow.

ABSTRACT

Specification of dorsal/ventral regional identity in progenitors of the developing telencephalon is a first pivotal step in the development of the cerebral cortex and basal ganglia. Previously, we demonstrated that the two zinc finger *doublesex and mab-3 related* (*Dmrt*) genes, *Dmrt5* (*Dmrta2*) and *Dmrt3,* which are coexpressed in high caudomedial to low rostrolateral gradients in the cerebral cortical primordium, are separately needed for normal formation of the cortical hem, hippocampus and caudomedial neocortex. We have now addressed the role of *Dmrt3* and *Dmrt5* in controlling dorsal/ventral division of the telencephalon in mice of either sex by comparing the phenotypes of single knock-out (KO) with double KO embryos and by misexpressing *Dmrt5* in the ventral telencephalon.

We find that DMRT3 and DMRT5 act as critical regulators of progenitor cell dorsoventral identity by repressing ventralizing regulators. Early ventral fate transcriptional regulators expressed in the dorsal lateral ganglionic eminence such as *Gsx2* are upregulated in the dorsal telencephalon of *Dmrt3;Dmrt5* double KO embryos and downregulated when ventral telencephalic progenitors express ectopic *Dmrt5*. Conditional overexpression of *Dmrt5* throughout the telencephalon produces gene expression and structural defects that are highly consistent with reduced GSX2 activity. Further, *Emx2; Dmrt5* double KO show a phenotype similar to *Dmrt3; Dmrt5* double KO embryos, and both DMRT3, DMRT5 and the homeobox transcription factor EMX2 bind to a ventral telencephalon-specific enhancer in the *Gsx2* locus. Together, our findings uncover cooperative functions of DMRT3, DMRT5 and EMX2 in dividing dorsal from ventral in the telencephalon.

SIGNIFICANCE STATEMENT

We identified the DMRT3 and DMRT5 zinc finger transcription factors as novel regulators of dorsoventral patterning in the telencephalon. Our data indicate that they have overlapping functions and compensate for one another. The double but not the single knockout produces a dorsal telencephalon that is ventralized, and olfactory bulb tissue takes over most remaining cortex. Conversely, overexpressing *Dmrt5* throughout the telencephalon causes expanded expression of dorsal gene determinants and smaller olfactory bulbs. Furthermore, we show that the homeobox transcription factor EMX2 that is coexpressed with DMRT3 and DMRT5 in cortical progenitors cooperates with them to maintain dorsoventral patterning in the telencephalon. Our study suggests that DMRT3/5 function with EMX2 in positioning the PSB boundary by antagonizing the ventral homeobox transcription factor GSX2.

INTRODUCTION

The mammalian telencephalon is the largest and most complex region of the mammalian brain, controlling cognitive processes and purposeful actions. It comprises the cerebral cortex dorsally and the amygdala and basal ganglia structures ventrally. Defects in telencephalon development are associated with many human neuropsychiatric and neurological disorders (Gaitanis and Walsh, 2004; Hu et al., 2014). Related to this study, a

loss-of-function mutation in the human *DMRT5/DMRTA2* gene has been found to be associated with microcephaly (Urquhart et al., 2016).

Specification of dorsoventral (DV) regional identity in progenitors of the developing telencephalon is a pivotal step in the development of the cerebral cortex and basal ganglia. In the developing telencephalon, as in the spinal cord, Bone Morphogenetic Proteins (BMPs) and Wingless-Int proteins (WNTs) produced dorsally and Sonic Hedgehog (SHH) secreted from ventral sources are implicated in DV specification of the telencephalon (Ericson et al., 1995; Chiang et al., 1996; Backman et al., 2005; Fernandes et al., 2007). Opposition between these morphogens alone does not establish DV telencephalic identity. Rather, interactions among the transcription factor GLI3, Fibroblast Growth Factor (FGF) signaling from the rostral telencephalic patterning center (RTPC), and ventral sources of SHH, regulate DV patterning (Ohkubo et al., 2002; Shimogori et al., 2004; Hasenpusch-Theil et al., 2017). GLI3 is a transcriptional activator in the presence of high levels of SHH, and a repressor, GLI3R, when levels of SHH are low (Grove et al., 1998; Theil et al., 1999; Tole et al., 2000a; Aoto et al., 2002; Kuschel et al., 2003). SHH promotes ventral identity by maintaining FGF signaling at the RTPC in part by suppressing formation of Gli3R which represses *Fgf8* expression (Ohkubo et al., 2002; Rallu et al., 2002; Rash and Grove, 2007). FGFs at the RTPC are in turn required to establish or maintain *Shh* expression in the ventral telencephalon (Storm et al., 2006). FGF signaling further promotes ventral telencephalon development independently of SHH, through regulating expression of the *Foxg1* transcription factor gene (Gutin et al., 2006; Tole and Hébert, 2013). *Pax6* and other homeobox genes such as *Emx2* (Muzio et al., 2002b, a) expressed throughout the pallium, and the homeobox gene *Gsx2* expressed in the subpallium are also involved in positioning the pallium-subpallium boundary (PSB) (Stoykova et al., 2000; Toresson et al., 2000; Yun et al., 2001; Kroll and O'Leary, 2005; Carney et al., 2009). How these different transcription factors function together to control telencephalon DV patterning and whether there are other players involved remains unknown.

Dmrt3 and *Dmrt5* (*Dmrta2*) encode related transcription factors expressed in a similar high caudomedial to low rostrolateral gradient in the cortical primordium. Their loss leads to a similar phenotype, more severe in *Dmrt*5 than in *Dmrt3* mutants. In either single null mutant, Wnt and BMP expression at the cortical hem is decreased and adjacent hippocampus and caudal neocortical areas are reduced in size. In conditional *Dmrt5* mouse models, *Dmrt5* loss or gain of function after hem formation also leads to a reduction of hippocampal size and alters neocortical area map formation, indicating that DMRT5 is not only required for hem formation but also directly controls cortical progenitor proliferation and specification. DMRT3 and DMRT5are thus crucial regulators of cortical development, acting at different steps of its formation (Konno et al., 2012; Saulnier et al., 2013; Young et al., 2017; De Clercq et al., 2018). DMRT3 and DMRT5 have similar DNA binding properties (Murphy et al., 2007) suggesting they act redundantly in telencephalic development, implying that analysis of single KO embryos did not reveal their full function. We therefore generated double KO and compared their telencephalic development with that of single KO embryos. Further, we conditionally overexpressed *Dmrt5* in the telencephalon. As *Emx2* is coexpressed with *Dmrt3* and *Dmrt5* in cortical progenitors, we also generated *Dmrt5;Emx2* double KO embryos. Our new findings reveal that DMRT3, DMRT5 and EMX2 cooperate to repress *Gsx2* and maintain DV patterning in the telencephalon.

MATERIAL AND METHODS

Animals.

All mice were maintained on a C57/Bl6 or CD1/C57Bl6 mixed background and mice of either sex were used. Midday of the day of the vaginal plug discovery was defined as embryonic day (E) 0.5.Animal care was in accordance with Institutional guidelines, and the policies of the US National Institutes of Health.

Dmrt3 (Saulnier et al., 2013), *Dmrt5* (De Clercq et al., 2018), *Emx2* (Pellegrini et al., 1996) and *Gsx2EGFP* mice (Wang et al., 2009) were genotyped by polymerase chain reaction (PCR) as described respectively in these articles. *Dmrt3+/-* or *Dmrt3-/-* animals, which are viable, were crossed with *Dmrt5+/-* mice to obtain *Dmrt3+/- ;Dmrt5+/-* mice. These double heterozygotes were then crossed to obtain *Dmrt3- /- ;Dmrt5-/-* homozygous double KO embryos. *Dmrt5-/-;Emx2-/-* homozygous double mutants were obtained by intercrossing *Dmrt5+/-* heterozygous mutants with *Emx2+/-* heterozygous mutants. *Dmrt5* conditional transgenic *(Dmrt5Tg*) mice were maintained and genotyped as described (De Clercq et al., 2018) and crossed to *Foxg1-IRES-Cre* (Kawaguchi et al., 2016) mice to overexpress *Dmrt5* throughout the telencephalon or to *Gsx2-Cre-IRES-EGFP* (*Gsx2-CIE*) (Qin et al., 2016) to overexpress it in ventral telencephalon progenitors. *tetO-Gsx2-IRES-EGFP mice* were crossed to *Foxg1TA/+* mice to obtain *Foxg1TA/+;tetO-Gsx2-IRES-EGFP* embryos overexpressing *Gsx2* throughout the telencephalon (Waclaw et al., 2009).

Histology, immunofluorescence and in situ hybridization.

Standard hematoxylin and eosin (H&E) staining was performed on 6–8 µm sections of embryosor brains fixed overnight in 4% paraformaldehyde/PBS, dehydrated and paraffin-embedded. For immunofluorescence, embryos were fixed overnight at 4°C in 4% paraformaldehyde/PBS, infused in 30% sucrose/PBS overnight, frozen in gelatin (7.5% gelatin, 15% sucrose/PBS) or NEG-50 and cryosectioned (12-20 µm). Antigen retrieval was performed by boiling the sections in Target Retrieval Solution Citrate pH 6.0 (DAKO®). Slides were the blocked with 10% normal goat serum, 0.3% Triton X-100 in PBS and incubated with primary antibodies O/N at 4°C. The incubation with secondary antibodies was carried out for 2h at RT. Samples were then mounted in DAKO® mounting medium. The following primary antibodies were used: rabbit anti-TH (1:500, Immunostar), rabbit anti-DMRT5 (1:2000, (De Clercq et al., 2018)), rabbit anti-GSX2 (1:500, (Toresson et al., 2000)); mouse anti-ASCL1 (1 :100, gift from C. Parras laboratory); goat anti-PAX6, (1:200, Santa Cruz); rabbit anti-TBR2 (1/500, Abcam) and chicken anti-GFP (1:1000, Aves Labs). The following secondary antibodies were used: anti-Mouse AlexaFluor 488 (1 :400, Invitrogen), anti-Mouse AlexaFluor 594 (1 :400,Invitrogen), anti- Rabbit AlexaFluor 488 (1 :400, Invitrogen), anti-Rabbit AlexaFluor 488 (1 :400, Invitrogen), anti- Rabbit AlexaFluor 594 (1 :400, Invitrogen). Sections were counterstained with DAPI. Images were acquired with a Zeiss LSM 70 confocal microscope using ZenBlack® software or Nikon A1R GaAsP inverted Confocal Microscope and processed using ImageJ and Photoshop® softwares.

In situ hybridization (ISH) on sections and whole-mount in situ hybridization of embryos were performed using antisense digoxigenin-labeled riboprobes as described (Saulnier et al., 2013; De Clercq et al., 2018). The other antisense probes were generated from the previously described cDNA clones: *Emx1* (Theil et al., 1999), *Ascl1* and Gad67 (Fode et al.,

2000), *Dlx2* (Porteus et al., 1991), *Gsx2* (Toresson et al., 2000) *Sp8* (Sahara et al., 2007) *Isl1* (Huber et al., 2013), *ER81* (Chotteau-Lelievre et al., 1997), *sFrp2* and *TGF-α* (Assimacopoulos et al., 2003). Images were acquired with an Olympus SZX16 stereomicroscope and a XC50 camera, using the Imaging software CellSens®.

Confocal imaging

Confocal imaging used a Zeiss LSM-710 confocal microscope using both Zeiss x10/0,3 EC Plan Neofluor and Zeiss x20/0,8 PlanApochromat objectives and with specific excitation using a 405nm laser diode, a 488nm Argon ion laser and a 594nm Helium/Neon laser. A specific Gallium arsenide phosphide (GaAsP) Airyscan detector was used when necessary to increase signal detection and signal/noise ratio. Images were acquired using Zeiss ZenBlack software (Zeiss, Oberkochen, Germany). For Tile scan imaging, acquisitions were performed with a 10% overlap of fields and images were reconstruct using ZenBlack software. For nuclei counting in Fig. 5, a homemade automated macro was developed on Fiji software. Briefly, background of images was reduced using a "rolling ball radius" function and nuclei were segmented through fluorescence intensity using an automated threshold. Nuclei segmented from both "green" and "red" channels were counted automatically through a size selection and nuclei present in both channels were considering as colocalizing. Brightness and contrast adjustments and image processing were done using Fiji and Photoshop software.

RNA sequencing.

RNA was extracted using the RNeasy mini kit from Qiagen (RNA-seq) and prepared for sequencing using the TruSeq RNA Sample Prep Kit v2. Four WT samples and five samples of each genotype were analyzed. Sequence reads have been obtained using an Illumina Hiseq 2000 in singleend mode (51bp). Sequencing quality was checked and approved using the FastQC software (http://www.bioinformatics.babraham.ac.uk/projects/fastqc/) and one *Dmrt5 KO* sample that had too low number of reads was removed. Reads were aligned to the mouse genome reference (genome assembly mm10 downloaded from ensembl.org) using the STAR alignment software (https://www.ncbi.nlm.nih.gov/pubmed/23104886, version 2.3) allowing for 2 mismatches within 51bp. Gene expression quantification was performed using the featureCounts tool (https://www.ncbi.nlm.nih.gov/pubmed/24227677). Count normalization and differential gene expression analyses were conducting using R/Bioconductor (version 3.2) and the DESeq2 package (https://www.ncbi.nlm.nih.gov/pubmed/25516281/, version 1.8.2). PCA and hierarchical clustering were applied to normalized count data. Two outlier samples were removed (one from control group after inspection of sample cluster plots and the one from the Dmrt5 KO group with low number of reads). Genes were annotated using the biomaRt package (https://www.ncbi.nlm.nih.gov/pubmed/19617889, version 2.24). Differentially expressed genes were selected based on a log2-fold-change and false discovery rate (FDR) cutoff of 1 and 0.05, respectively. Gene Ontology (GO) analysis was performed using DAVID 6.7 (http://david.abcc.ncifcrf.gov) in the annotation category BP-FAT. Strongly enriched categories had a score of 0.05 or less after Benjamini multiple test correction. RNAseq data have been deposited at NCBI GEO (GSE108611).

Plasmid construct and transgenesis

The 1.8 kb of the *Gsx2* locus (chr5: 75481187-75479361, mm9 assembly) was amplified by

polymerase chain reaction (PCR) with the oligonucleotides forward 5'-CGCACCGTTGGGGATTCTAA-3' and reverse 5' TCTCTCAATTCCCAGGGGTCA-3' and using DNA from BAC clone RP23-382i10 as template. The resulting fragment was subcloned 5' of the globin basal promoter in the SpeI and NotI sites of a reporter vector (BGZA) containing the chick □-globin promoter, the lacZ reporter gene, and an SV40 polyadenylation cassette (Yee and Rigby, 1993). The 1.3kb fragment of the *Gsx2* locus (chr5: 75480316-75481596, mm9 assembly) was amplified by PCR with the oligonucleotides forward 5'-GGCGCGCCCACCCTTTTGTTTTGTTGTTAAGACTTAG-3' and reverse 5' ACAAAAAAGCAGGCTGTTGTCGTTCAGGTGGCAAGG-3' using DNA from BAC clone RP24-223O21 as template, and was inserted into a vector containing *Cre-IRES-EGFP.* Transgenic embryos were generated by pronuclear injection at the Transgenesis platform of the De Duve Institute, UCL, Leuven using fertilized eggs from B6CBAF1/Crl crosses (for fragment A) or at the Transgenic Animal and Genome Editing Core at Cincinnati Children's Hospital Medical Center by microinjection of fertilized eggs from FVN mice (for fragment B). Transgenic embryos were identified by PCR using tail DNA. Expression of the transgene was analyzed in E12.5 embryos. LacZ activity in transgenic embryos was detected by whole mount X-gal staining. Expression of the GFP transgene was examined by DAB staining of a E12.5 brain sections with chicken anti-GFP antibodies (1:1000, Aves Labs), followed by biotinylated donkey anti-chicken IgY (1:200, Jackson Immunoresearch) and ABC solution (Vector Laboratories).

Electrophoretic mobility shift assay.

Electrophoretic mobility shift assays were performed using extracts from HEK293 cells transfected with *Dmrt3*, *Dmrt5* and/or *Emx2* pEFX expression vectors. The double stranded oligonucleotide used containing the Dmrt and/or Emx2 binding sites (underlined) were the following: Dmrt BS1: 5'-GCTGGGTTACACTGGAAGGA-3'; Dmrt BS2: 5' TAGTCACTGTTTCATTAGGC- 3'; Dmrt BS3: 5'-GACTTTTCGATACATTCCTA-3'; Emx2 BS1: ACCTCCCCTCTTCCTTCCTAATTAATGACCAT-3'; DMRT BS3/EMX2 BS2: 5' GACTTTTCGATACATTCCTAATTGACTGAGGG-3'. Briefly, double stranded biotin-labelled probes and non-labelled competitors were prepared by mixing equal molar ratio of two complimentary oligos in Annealing buffer (10 mM Tris-HCl pH7.9, 10 mM $MgCl_2$ and 50 mM NaCl). The paired oligos were heated to 95°C for 5 min then the temperature were reduced slowly to room temperature on hot blot. DNA binding reaction was performed in Binding buffer (10 mM Tris-acetate pH7.9, 5 mM Magnesium acetate, 25 mM Potassium acetate, 0.1 □M ZnSO4 and 50 µg/ml BSA) including 0.5□□g sonicated herring sperm DNA and 1pmole double stranded DNA probe. Twenty-three pmoles of competitor (23 fold molar excess to probe) was used in each reaction as indicated. Protein-DNA complexes were separated by electrophoresis at 50V for 3 hrs on 5% polyacrylamide mini gels in 0.5xTBE at 4°C. DNA was transferred to Hybond+ membrane using Bio-Rad Trans-Blot® SD Semi- Dry Electrophoretic Transfer Cell and crosslinked by UV light for 5 min. Biotin-labelled DNA was detected using the Thermo Scientific™ Pierce™ Chemiluminescent Nucleic Acid Detection Module.

Experimental design and Statistical analysis

Quantification of the dorsal surface area of the cortical hemisphere of E12.5 and E18.5 animals was obtained by taking measurements from images of whole brains. Photographs were taken with an Olympus SZX16 stereomicroscope and a XC50 camera. Measurements were done using ImageJ software. All quantified data are expressed as mean values ±

standard deviation (SD) with the value obtained for WT set to 1. Significance tests were performed using a 2-tailed Student's t-test; P-values less than 0.05 were regarded as statistically significant. For each genotype, at least 5 embryos were examined.

In *Dmrt* single and double KO and transgenic *Dmrt5* overexpressing embryos, for each marker and age, 2-4 embryos were analyzed. In *Dmrt5;Emx2* double mutants, markers were only examined in 2 embryos due to the difficulties of obtaining them. For each of the markers used and in embryos of the different genotypes analyzed, photographs of sections from the rostral to caudal or from the lateral to medial part of the telencephalic vesicles were taken and assembled into series. Comparable coronal sections, taken at rostral to mid telencephalon levels (based on landmarks provided by the ganglionic eminences), and sagittal sections, taken at the level of the olfactory bulb, are shown.

Mice with conditional misexpression of *Dmrt5* throughout the telencephalon (using the *Foxg1- IRES-Cre* driver line) show a ventral expansion of the normally dorsally expressed gene, *Emx1*. The amount of expansion was measured in images of coronal brain sections through E12.5 conditional transgenic and control embryos. Images were obtained with a Zeiss Axioscope microscope fitted with Axiovision software (Zeiss). Five 12.5 transgenic embryos and five controls, from three different litterswere utilized. To quantify the ectopic spread of *Emx1* expression, a consistent landmark between control and mutant mice was essential. The demarcation between the LGE and MGE was such a landmark, given that the MGE appeared essentially unaltered in *Dmrt5Tg/+;Foxg1IRES-Cre/+* embryos. We therefore measured how close the expression of *Emx1* came to this landmark, focusing on expression in the medial and central parts of the LGE where *Emx1* is not expressed in WT mice. Measurements were made using ImageJ, and the two groups were statistically compared with the Paired Sample Student's t-test.

For the transgenic embryos, X embryos were obtained positive 4 positive for construct B based on PCR results. Among them, possibly due to transgene integration into silent/closed locus, only two out of the 4 transgenic embryos for construct B, showed expression in the ventral telencephalon.

RESULTS

***Dmrt3;Dmrt5* double KO show greater defects in the cerebral cortex than either single KO Embryos**

We generated *Dmrt3;Dmrt5* double mutants by intercrossing the *Dmrt3* and *Dmrt5* single mutants (Konno et al., 2012; Saulnier et al., 2013; De Clercq et al., 2018). *Dmrt3;Dmrt5* double KO die at birth, as do *Dmrt5* single KO mice (Saulnier et al., 2013), therefore, embryos were analyzed just before birth (E18.5). We found that the dorsal surface area roughly correlated with the number of null *Dmrt3* and *Dmrt5* alleles in an individual genotype, such that cortical hemispheres in *Dmrt3;Dmrt5* double KO were strikingly smaller than either single KO embryos (-63+/- 3.4% compared to -43+/- 7.6% in *Dmrt5* KO and -13+/- 10.4% in *Dmrt3* KO embryos) (Fig. 1 A,B). This more severe reduction of the cerebral hemispheres in double KO embryos was already apparent at E12.5 (-52.5 +/- 0.04% compared to -43.7 +/- 0.06% in *Dmrt5* KO and to -19.9 +/-0.32% in *Dmrt3* KO embryos).

In *Dmrt3;Dmrt5* double KO, the reduction of caudal neocortical areas, hippocampus and other dorsomedial telencephalic structures, such as the cortical hem, is more dramatic than in single KO embryos (data not shown). An obvious external difference between single KO and *Dmrt3;Dmrt5* double KO embryos was that the telencephalic vesicles of the double KO embryos show no discernible olfactory bulb (OB) (Fig. 1 A,C). However, when analyzed with gene and protein expression markers of the OB, including *Tbx21* whose expression is limited to OB mitral cells (Faedo et al., 2002; Kahoud et al., 2014), the residual pallium of the double KO embryos appears dominated by an olfactory bulb-like structure (OBLS) (Fig. 1 D). Thus, the *Dmrt3;Dmrt5* double KO have more substantial defects than either single KO embryos, suggesting that *Dmrt3* and *Dmrt5* compensate for the loss of one another.

Loss of both *Dmrt3* and *Dmrt5* causes ventralization of the pallial neuroepithelium.
To determine how DMRT3 and DMRT5 interact to regulate gene expression in the developing telencephalon, we dissected the dorsal telencephalon from E12.5 *Dmrt3* KO, *Dmrt5* KO, *Dmrt3;Dmrt5* double KO and WT embryos and carried out a transcriptome analysis of the dissected tissue by RNA sequencing (RNAseq) (Fig. 2 A). Applying a minimal cutoff of twofold change and a significance level of $p<0.05$, 68 differentially expressed genes were identified in the *Dmrt3* single KO, 146 in the *Dmrt5* single KO embryos and 553 in the double KO embryos. The majority of differentially expressed genes were downregulated (67 in *Dmrt3* KO, 126 in *Dmrt5* KO and 422 in *Dmrt3;Dmrt5* double KO) and the overlap between the single and double KO embryos was very high (Fig. 2 A). Gene ontology (GO) analysis of the deregulated genes identified in the double KO embryos revealed an enrichment in genes involved in neuron differentiation, forebrain development, neuron fate and cell fate commitment (data not shown). Among the down-regulated genes in the double KO embryos were, as expected (Saulnier et al., 2013; De Clercq et al., 2018), genes of the WNT and BMP signaling pathways associated with the cortical hem, and downstream targets genes linked to hippocampus and choroid plexus development (*Wnt3a*, *Bmp6*, *Lmx1*, *Emx1*, *Lhx2*, *Nfix*, *Rspo1-3*, *Foxj1*, *Ttr*, *Mcidas*, *Gmnc*, *Ccno*, *Dnah6*). Partially overlapping this list, were transcription regulators of dorsal telencephalic fates, including *Emx1*, *Emx2*, *Lhx2*, *Tbr2/Eomes*, the proneural factors *Ngn2/Neurog2*, *NeuroD1*, *Math2*/*NeuroD6*, *Nhlh1* and the glutamatergic neuronal gene *Vglut1*. Among upregulated genes were unexpectedly, many transcriptional determinants of ventral telencephalic cell fates, including *Gsh2/Gsx2, Dlx2, Dlx5, Sp8, Sp9, Ascl1*, ventral neuronal telencephalic genes (*Gad1/Gad67, Gad2, Scl30a3, Slc32a1*) and olfactory bulb interneuron genes (*Foxp2, TH, calbindin*) (Fig. 2 B,C). The dorsal determinant *Pax6* was also slightly increased, but its change of expression level was below the applied twofold change cutoff. Genes encoding general regulators of neurogenesis such as *MyT1, Myt1l*, and general neuronal markers (*Dcx, Mapt, Nefh*) were, in contrast, not differentially expressed. The most highly up- and down-regulated genes together with the change of their expression in the different KO genotypes are shown in Fig. 2 B,C. For the vast majority of the deregulated genes identified, the changes observed in the *Dmrt3; Dmrt5* double KO embryos relative to WT controls were in the same direction as those observed in the two single KO embryos, suggesting that *Dmrt3* and *Dmrt5* are redundant in several aspects of cortical development. The changes were generally greater than additive and the deregulation observed in *Dmrt5* KO was always much stronger than in *Dmrt3* KO embryos. For a given target, the difference between the WT and *Dmrt3* KO expression levels (EWT -EDmrt3 KO) and between the *Dmrt5* KO and *Dmrt3; Dmrt5* double KO (EDmrt5KO -EDmrt3/5 DKO) represent the contribution of *Dmrt3* to gene expression in

the presence or absence of *Dmrt5*. For many of the transcripts, this EWT -EDmrt3 KO value is smaller than the EDmrt5KO - EDmrt3/5 DKO value. The greater effect of the loss of *Dmrt3* in the double KO embryos than in the WT context suggests that *Dmrt5* indeed partially compensates for the loss of *Dmrt3*.

Distinct domains are distinguished in the early telencephalic neuroepithelium (Fig. 3). The dorsal telencephalon, or pallium, is subdivided into the medial, dorsal, lateral and ventral pallium (MP, DP, LP and VP). MP generates the hippocampus, and the DP gives rise to the neocortex. The LP and the VP contribute neurons to olfactory cortex and the amygdala. The ventral telencephalon, or subpallium, has three proliferative subdomains, the lateral, medial and caudal ganglionic eminences (LGE, MGE and CGE), which develop into the striatum, globus pallidus and parts of the amygdala. The MGE and CGE are also the source of GABAergic interneurons, which migrate tangentially into the cortex (Anderson et al., 1997; Puelles et al., 2000; Flames et al., 2007). To confirm the differential gene expression revealed by the RNA-seq analysis, we performed *in situ* hybridization of selected deregulated genes on brain sections of E12.5 embryos (Fig. 3). We first examined patterning genes such *Emx1, Emx2*, *Pax6 and Ngn2,* expressed in the cortex of wild-type (WT) mice, and *Dbx1* expressed selectively in the VP, which lies adjacent to the pallial-subpallial boundary (PSB) (Fig. 3A). For genes expressed in the subpallium, we analyzed *Gsx2, Dlx2* and *Ascl1* (Toresson et al., 2000; Yun et al., 2001; Tole et al., 2005).

The dorsal regulators *Emx1, Emx2* and *Ngn2* were strongly decreased in cortical progenitors of the double KO, more severely than in either single KO embryos. Expression of these genes remained detectable only in the dorsomedial telencephalon (Fig. 3A, open arrows). *Dbx1* expression which remains detectable in the VP of both single KO embryos was lost in the double KO embryos (Fig. 3A, open arrow). In contrast, *Pax6*, which is upregulated in the cortex of *Dmrt* single KO (Saulnier et al., 2013; De Clercq et al., 2018), remained expressed in the cortex of the double KO embryos but was reduced at the PSB. *Gsx2, Dlx2* and *Ascl1* whose expression is restricted to the subpallium in WT embryos, extended dorsally into the lateral part of the telencephalon in the double KO (arrows in Fig. 3A), a phenotype that was not observed in either single *Dmrt* KO embryos.

The LGE is subdivided into a dorsal (dLGE) and a ventral domain (vLGE) (Yun et al., 2001). dLGE progenitors express *Sp8* and generate olfactory bulb interneurons, whereas vLGE progenitors express *Isl1* and give rise to striatal GABAergic projection neurons (Stenman et al., 2003; Waclaw et al., 2006; Waclaw et al., 2009; Ehrman et al., 2013). We examined their expression in single and double KO embryos. *Sp8*, normally restricted to the dLGE SVZ, showed a similar expression in single KO, but expanded dorsally the double KO embryos (Fig. 3B, arrow). *Isl1* expression in single KO embryos was similar to WT controls. In double KO, *Isl1* appears only moderately affected, with only very weak staining detectable in the cortex (Fig. 3B).

We also examined expression of dorsal and ventral regulator genes in sagittal sections (Fig. 4). Expression of *Ngn2* and *Emx1* retracted caudodorsally. *Pax6* expression, upregulated in the single KO, also appeared to retract in double KO embryos. This was accompanied by a dorsal expansion of *Gsx2* and *Dlx2* expression in the anterior telencephalon. In the brain of E12.5 *Dmrt3; Dmrt5* double KO embryos, subpallial gene expression expand dorsally both in

the lateral and anterior telencephalon (Fig. 4, arrows). We found that *Er81* expression, restricted at E12.5 in WT embryos to the olfactory bulb primordium (OBP) (Stenman et al., 2003; Allen et al., 2007; Besse et al., 2011), was also extensively expanded caudally (Fig. 4, arrow). Together, these results indicated that in E12.5 *Dmrt3; Dmrt5* double KO, there is an expansion of dLGE and OBP domains, as characterized by gene expression, into the dorsal telencephalon, and a concomitant shrinkage of the dorsal pallium (Fig. 1C and 3C).

The expansion of dLGE and OBP domains in E12.5 *Dmrt3; Dmrt5* double KO could be the consequence of the collapse of the dorsal telencephalon and invasion of ventral progenitors or of a respecification, namely ventralization of dorsal telencephalic progenitors. To test the second hypothesis, we performed double immunostaining with antibodies for both the dorsal PAX6 and ventral GSX2 markers on coronal brain sections of E12.5 single and double KO embryos and WT controls. In the lateral cortex of the double KO embryos, but not in the single KO and WT embryos, many cells were found to be positive for both markers (Fig. 5), suggesting that indeed dorsal telencephalic progenitors were acquiring a ventral identity, perhaps corresponding to that in WTs of the few cells present at the PSB that coexpress *Pax6* and *Gsx2*, or a hybrid fate.

To assess the consequences of the ventralization of dorsal progenitors in *Dmrt3;Dmrt5* double KO embryos, we examined Tyrosine hydroxylase (TH), found in a subpopulation of OB interneurons, *Gad67*, a GABAergic interneuron marker, and *Math2*, a marker of glutamatergic cortical neurons in sagittal sections of E18.5 brains. In accordance with our observation of an expansion of the dLGE and OBP at E12.5, compared to single KO and controls, TH-positive cells were detected more caudally and *Gad67* was increased in the dorsal telencephalon of the double KO embryos. Compared with single KO and controls, *Math2* expression was in contrast dramatically reduced overall (Fig. 6), suggesting some respecification of cortical neuroblasts.

Misexpression of *Dmrt5* in the subpallium represses ventral telencephalic markers

To perform *Dmrt5* gain-of-function experiments, we used a *Dmrt5 Cre/loxP* conditional transgenic mouse model we recently generated. In our previous work, the *Dmrt5* conditional transgenics (designated here *Dmrt5Tg* mice) were crossed with *Emx1-Cre* mice to study the role of DMRT5 in neocortical area map formation (De Clercq et al., 2018). *Emx1-Cre* drives excess *Dmrt5* only in the dorsal, not ventral telencephalon, and Cre lox recombination begins in the most medial telencephalon at roughly E10, spreading laterally so that full recombination in lateral cortex is as late as E11.5. In the present study, *Dmrt5Tg* mice were crossed with different Cre driver lines, *Foxg1-IRES-Cre* or *Gsx2- Cre-IRES-EGFP* (*Gsx2-CIE*). In *Dmrt5Tg/+;Foxg1IRES-Cre/+* embryos, *Dmrt5* is overexpressed in both the dorsal and ventral telencephalon from E8.5 (Kawaguchi et al., 2016), thus much earlier and more broadly than with *Emx1-Cre*. In *Dmrt5Tg/Tg;Gsx2-CIE* embryos, *Dmrt5* is overexpressed selectively in the ventral telencephalon from E10.5 (Qin et al., 2016).

As expected, in *Dmrt5Tg/+;Foxg1IRES-Cre/+* embryos, *Dmrt5* transgene expression detected by GFP ISH filled the entire telencephalon (data not shown). In E12.5 *Dmrt5Tg/+;Foxg1IRES-Cre/+* embryos, we examined the expression of ventral (*Gsx2*, *Dlx2* and *Ascl1*) and dorsal (*Emx1* and *Ngn2*) telencephalic markers. We also analyzed *sFrp2*, *Tgf-α*, *Dbx1* expressed in the VP (Assimacopoulos et al., 2003) and *Sp8* marking the dLGE (Fig. 7).

In E12.5 control embryo sections, *Emx1* expression did not enter the LGE and only extended along the far lateral edge of the LGE in a territory that may be presumptive olfactory cortex. By contrast, in *Dmrt5Tg/+;Foxg1IRES-Cre/+* E12.5 embryos, the *Emx1* expression domain expanded ventrally into the central and medial LGE (Fig. 7A, arrow). This expansion of *Emx1* expression in *Dmrt5Tg/+;Foxg1IRESCre/+* E12.5 embryos, compared with controls, was quantified by measuring how close the central sector of *Emx1* expression came to the boundary between the LGE and the MGE. The latter boundary served as a consistent landmark because the MGE appeared morphologically unaffected by overexpression of *Dmrt5*. For *Dmrt5Tg/+;Foxg1IRES-Cre/+* E12.5 embryos the mean distance from the *Emx1* expression front and the LGE/MGE boundary was 133.3 microns (SEM, 25.3; SD 75.9), and for control embryos, 273.8 microns (SEM, 18.2; SD, 54.6). The two groups were significantly different (p=0.0004). Notable by eye, but not quantified, the extension of *Emx1* expression increased from rostral to caudal, reaching the MGE/LGE boundary in more caudal sections. Similarly, *Ngn2* expression, normally confined to the cerebral cortical primordium, expanded into almost all the LGE territory (Fig. 7A, arrow).

In contrast, *Gsx2 and Dlx2* expression was downregulated overall and did not reach along the entire DV length of the LGE (Fig. 7A, arrow). The strongest expression of both *sFrp2* and *Tgf-α* was shifted ventrally and *Sp8* in the dLGE was virtually absent (Fig. 7A, arrow). At E13.5, *Tgf-α* and *sFrp2* appeared to have recovered a normal expression level at the PSB, but expression of *Dbx1*, a selective marker of the VP, was greatly expanded and shifted ventrally. *Sp8* remained virtually absent in the dLGE (Fig. 7B, arrow). Thus, at E13.5, the PSB boundary expressed some appropriate genes, yet the VP area as marked by *Dbx1* had expanded (Fig 7C). An enlarged VP was previously observed in the *Gsx2* null mutant (Yun et al., 2001; Carney et al., 2009; Waclaw et al., 2010).

Sp8 in the dLGE is required for OB interneurons to begin migration through the embryonic rostral migratory stream (Waclaw et al., 2006). In *Dmrt5Tg/+;Foxg1IRES-Cre/+* brains at P6, consistent with the virtual loss of *Sp8* expression in the dLGE, the ventricle of the OB was slightly open rather than filled with migrating interneurons as in WT mice, suggesting that interneurons were not reaching the OB correctly (Fig. 7D).

In *Dmrt5Tg/Tg;Gsx2-CIE* embryos, *Dmrt5* overexpression was only detected in the ventral telencephalon, as expected. As observed in *Dmrt5Tg/+;Foxg1IRES-Cre/+* embryos, *Dmrt5* ectopic expression induces loss of the ventral (*Gsx2, Dlx2, Ascl1)* and gain of the dorsal (*Emx2, Ngn2*, *Dbx1*) markers tested (Fig. 8), suggesting that the ventral expansion of dorsal telencephalic and ventral pallium markers is largely caused by the downregulation of ventral determinants.

EMX2 interacts with DMRT5 to control telencephalic D/V patterning and both transcription factors can bind to a ventral telencephalic-specific enhancer of the *Gsx2* locus.

Emx2 is coexpressed with *Dmrt3* and *Dmrt5* in cortical progenitors in a similar graded manner. As in *Dmrt5* or in *Dmrt3* single mutants, the hippocampus and caudomedial neocortex are reduced in *Emx2* deficient mice (Yoshida et al., 1997; Tole et al., 2000b). This reduction too is more dramatic in *Dmrt5/Emx2* double KO than in single KO embryos (Fig.

9A), suggesting that *Dmrt5* and *Emx2* genes interact in controlling telencephalic growth and patterning. Supporting such an interaction, *in situ* hybridization showed that in E12.5 *Dmrt5/Emx2* double KO brains, the pallial transcription factor gene *Ngn2* was switched off whereas gene expression domains of *Gsx2, Dlx2* and *Ascl1*, normally confined to the subpallium, extended dorsally, a phenotype not observed in either *Dmrt5* or *Emx2* single KO embryos (Fig. 9B).

GSX2 is crucial for ventral identity in the telencephalon. In *Gsx2* mutants, the VP expands into the dLGE (Toresson et al., 2000; Yun et al., 2001; Carney et al., 2009; Waclaw et al., 2010). Conversely, *Gsx2* misexpression in the pallium results in increased expression of ventral telencephalic markers and repression of dorsal ones (Toresson et al., 2000; Yun et al., 2001; Carney et al., 2009; Waclaw et al., 2009), including *Dmrt5* (Fig. 10).

To investigate how GSX2 and DMRT5 interact, we first compared by immunofluorescence their expression in *Gsx2GFP/+* knock-in embryos and found that the two proteins abut at the PSB (Fig. 10). Their exclusive expression at the PSB, the upregulation of *Gsx2* observed in *Dmrt3;Dmrt5* and *Dmrt5;Emx2* double KO embryos, along with its downregulation in response to overexpression of *Dmrt5*, suggest that DMRT5 may regulate cortical identity in telencephalic progenitors via repression of *Gsx2* transcription. We therefore searched the *Gsx2* locus for non-coding, evolutionarily conserved potential enhancer sequences (Bejerano et al., 2004; Pennacchio et al., 2006) with potential DMRT3/5 binding sites (Murphy et al., 2007). We focused on one such conserved site of about 0.5 kb that has been described as an enhancer bound by PAX6 that is active in the forebrain but not the lens (Sun et al., 2015), and is located 8.8 kb downstream of *Gsx2* transcribed sequences. Two overlapping fragments, encompassing this conserved region, one of 1.8kb including upstream sequences and the other of 1.3 kb containing downstream sequences and including another conserved region (respectively fragments A and B, Fig 11A) were cloned and fused to a reporter gene (constructs A and B). We found that both fragments tested exhibit specific enhancer activity in the ventral forebrain in E12.5 transgenic embryos, suggesting that it is the conserved region common to the two fragments that is responsible for the activity (Fig. 11B). This conserved region contains two potential DMRT3/5 binding sites (BS) as well as one 5'-ATTA-3' which represent the core of potential homeobox transcription factor–binding motifs (Berger et al., 2008). This 5'-ATTA-3'motif is adjacent to the second Dmrt3/5 BS. Upstream of this conserved region, within the cloned genomic fragments, we found one additional Dmrt3/5 BS and one additional 5'-ATTA-3' motif (Fig. 11A). To test for direct binding of DMRT3/5 and EMX2 to these putative binding sites, we performed electrophoretic mobility shift assays (EMSA) using extracts prepared from HEK293 cells transfected with *Dmrt3*, *Dmrt5* or *Emx2* expression plasmids. In first EMSA assays, using oligonucleotides containing the different Dmrt and Emx2 potential binding sites, we found that DMRT5 and DMRT3 both bind strongly to binding site 3 but not to the other sites. EMX2 can bind to both identified binding sites (data not shown). We then examined the ability of DMRT3, DMRT5, and EMX2 to bind to an extended oligonucleotide encompassing both Dmrt BS3 and Emx2 BS2, in the presence or absence of an identical competitor oligonucleotide containing mutated Dmrt and Emx2 binding sites. Fig 11C shows that, as expected, the binding of DMRT3, DMRT5 and EMX2 to the Dmrt BS3/Emx2 BS2 oligonucleotide is abolished in the presence of WT but not mutated competitors. Interestingly, in the presence of EMX2, the complex of DMRT3 appears more intense and

to run faster than in its absence. Although no change in mobility shift was observed, DMRT5 binding in the presence of EMX2 appears also more intense than in its absence, suggesting cooperative interactions between DMRT3/5 and EMX2.

DISCUSSION

We have previously identified DMRT5 and DMRT3 as important regulators of the development of caudomedial cortical structures acting downstream of dorsal WNT midline signals and controlling *Wnt* expression in a feedback loop (Hasenpusch-Theil et al., 2012; Saulnier et al., 2013; De Clercq et al., 2018). In the present study, we show that the size of the cortical hemispheres is drastically smaller in the *Dmrt3;Dmrt5* double KO than in the single KO embryos, further highlighting their importance in the control of the proliferative state of progenitor cells. This dramatic reduction in size of the cortex of the double KO embryos may due to premature differentiation and exhaustion of the pool of progenitors as observed in *Dmrt5-/-* embryos (Young et al., 2017), which remains to be explored. We also show that the development of caudomedial telencephalic structures such as the cortical hem and hippocampus is more severely reduced in the *Dmrt3;Dmrt5* double KO than in the single KO embryos. Together, these observations indicate that DMRT3 and DMRT5 have similar overlapping function in several aspects of cortical development and partially compensate for one another. *Dmrt5* is upregulated in the absence of *Dmrt3* and *Dmrt3* is downregulated in *Dmrt5* KO embryos. The two factors appear thus to function in the same cascade but it remains unclear which one is upstream of the other.

More unexpected, we observed that double knock-outs have a dorsal telencephalon that is ventralized. In addition the olfactory bulbs, the most rostral cortical structure, take over the cortex, thus suggesting “rostroventralization” of the dorsal telencephalon, in accordance with the high caudal to low rostral gradient of expression of *Dmt3/5* genes. Conversely, in *Dmrt5* overexpressing embryos, DP genes expand ventrally, although some PSB markers remain in place, and olfactory bulbs are smaller than in wildtype mice. In addition, *Dbx1* expression expands supporting an expansion of the VP. These findings revealed a new early role for DMRT5 and DMRT3 in DV telencephalic patterning, that could not have been predicted from examining the phenotype of either single KO line alone. This role fits with the timing of activation in the developing telencephalon. Both *Dmrt3* and *Dmrt5* expression is detected from the open neural plate stage in the prospective dorsal telencephalon when patterning is initiated (data not shown).

As noted, WNT and BMP signaling molecules and downstream dorsal telencephalic transcription factors are dramatically reduced in the cortex of the double KO embryos. The reduction of these pathways is likely to be involved in the ventralization. In contrast, FGF signals appears unaffected and SHH and downstream targets such as *Nkx2.1* appear normally restricted to the MGE (data not shown). Gli3R is another major player in telencephalic DV patterning (Theil et al., 1999; Tole et al., 2000a; Rallu et al., 2002; Kuschel et al., 2003). RNA-seq analysis of the cortex of E12.5 single and double *Dmrt* KO embryos did not detect a significant difference in *Gli3* mRNA levels compared with WT controls. This unaltered expression of *Gli3* in double *Dmrt* KO embryos has been confirmed by *in situ* hybridization and RT-qPCR experiments (data not shown). Given the similarity of the telencephalic patterning defects observed in *Dmrt3;Dmrt5* and *Gli3Pdn/Pdn* mutants, whether a reduction of Gli3R activity occurs in the *Dmrt* double KO embryos is an hypothesis

that remains to be tested. A more significant role in the ventralization of double *Dmrt* KO ermbryos is likely to be played by the transcription factor GSX2. In the ventral telencephalon, GSX2 is known to be required for the specification of LGE progenitors. GSX2, further, represses the expression of *Dbx1* and other VP markers (Yun et al., 2001; Carney et al., 2009). Our data indicate that it also represses *Dmrt5* expression. GSX2 acts in the specification of LGE progenitors upstream of the homeobox *Dlx* and proneural *Ascl1* genes (Wang et al., 2009; Wang et al., 2013). Thus, the increase of *Dlx2* and *Ascl1* and the loss of dorsal and ventral pallium markers in *Dmrt3;Dmrt5* double KO embryos may be a consequence of the dorsal expansion of *Gsx2*. The large expansion of *Gsx2* and other subpallial markers in the cortical neuroepithelium when *Dmrt3* and *Dmrt5* are lost is intriguing because it occurs despite continued strong *Pax6* expression in the cortex, which is reduced only close to the PSB. PAX6 has been shown to repress *Gsx2* expression to position the PSB (Toresson et al., 2000; Yun et al., 2001; Carney et al., 2009) but PAX6 may be not sufficient for this role in the absence of DMRT3 and DMRT5.

Gsx2 is expressed at high level in dLGE progenitors that generate *ER81* and *Sp8* expressing olfactory bulb interneurons, and at lower levels in vLGE progenitors giving rise to *Isl1* expressing striatal projection neurons (Toresson and Campbell, 2001; Yun et al., 2001; Stenman et al., 2003; Waclaw et al., 2006; Ehrman et al., 2013). *Gsx2* mutants have reduced vLGE and dLGE and exhibit a significant reduction of their derivatives, striatal projection and olfactory bulb interneurons (Corbin et al., 2000; Toresson et al., 2000; Yun et al., 2001; Yun et al., 2003). Conversely, in *Gsx2* conditional transgenics, GSX2 sequentially favors striatal and olfactory bulb fates (Waclaw et al., 2009). In *Dmrt* double KO embryos, we observed at E12.5 strong ectopic expression of *Sp8* but no or low *Isl1* indicating a predominant expansion of dLGE. Accordingly, at E18.5, TH positive interneurons appear abundant in the OBLS structure and Gad67, expressed in OB interneurons, is increased. At the same stage in the double mutant cortex, we also observed a strong reduction of *Math2* suggesting that some respecification of cortical neuroblast is occuring as a consequence of the observed early patterning defects.

Upon ectopic expression of *Dmrt5* throughout the telencephalon, we observed at E12.5-E13.5 a loss of *Gsx2* expression and downstream dLGE gene expression markers, and an expansion of DP and some VP gene expression markers into the subpallium. Other PSB markers appeared less affected. *SFrp2* expression shifted ventrally at E12.5, but recovered at E13.5. In *Gsx2* mutants, a strong LGE phenotype at early stages goes away later, due to increased *Gsx1* expression (Toresson and Campbell, 2001; Yun et al., 2003; Carney et al., 2009). Whether there is a compensatory increase in *Gsx1* in the *Dmrt5Tg/+;Foxg1-IRES-Cre* that rescues the location of *sFrp2* expression remains to be investigated. An alternative possibility is that the PSB repositions itself. The VP, however, does not, and instead expands in subpallial territory, thus dissociating the VP from the PSB. A similar dorsalizing phenotype was observed when *Dmrt5* is selectively misexpressed in the ventral telencephalon. This indicates that the ventral expansion of DP and VP gene expression markers is indirect and caused by downregulation of ventral determinants by DMRT5. Gsx2 is again a good DMRT3/5 target candidate as *SHH* and *Nkx2.1* were found to be unaffected in *Dmrt5Tg/Tg;Gsx2-CIE* embryos (data not shown). A further suggestion is that dorsal identity in the telencephalon is a “ground state” which must be suppressed by ventral determinants.

Finally, our findings indicate that *Emx2*, a target of *Dmrt5* (Saulnier et al., 2013), cooperates with *Dmrt3* and *Dmrt5* in repressing *Gsx2*, and that these transcription factors bind to an evolutionarily conserved, PAX6-bound element, located downstream of *Gsx2*. This *Emx2* involvement in *Dmrt*dependent *Gsx2* repression, echoes a previous report that co-ablation of *Emx2* and *Pax6* results into generalized spreading of subpallial programs into dorsal telencephalon and suppression of pallial programs (Muzio et al., 2002a). Intriguinigly, despite the prominent ventralization of dorsal telencephalon occurring in mid-neuronogenic *Emx2-/-;Pax6-/-* and *Dmrt3-/-;Dmrt5-/-* embryos, vestigial and abortive pallial specification can be still detected at earlier developmental stages in both double KO embryos.

In summary, our findings suggest that DMRT3/5 transcription factors and GSX2 mutually antagonize one another and that DMRT3/5 cooperate with EMX2 and PAX6 to establish and maintain dorsoventral patterning in the telencephalon. How DMRT3 and DMRT5 interact with EMX2, and possibly PAX6 and other dorsal regulators such as LHX2 to control the positioning of the PSB and, more globally, telencephalon patterning remains to be investigated.

FIGURE LEGENDS

Fig. 1 Cortices of *Dmrt3;Dmrt5* double KO embryos are more severely reduced in size than either single KO embryos and contain a prominent olfactory bulb-like structure. (A) Dorsal views of E18.5 brains of the indicated genotypes. (B) Quantification of dorsal cortical surface area compared to WT controls (in red) or as indicated (**p < 0.01, ***p < 0.001; n ≥5). (C) Diagram showing the telencephalon of E18.5 WT embryos and the size reduction and absence of the olfactory bulbs observed in *Dmrt3-/-;Dmrt5-/-*. (D) Sagittal sections through E18.5 brains processed by IF or ISH for *Tbr1*, Tbr2 and *Tbx21* olfactory bulb mitral projection neuron markers. In the cortex, Tbr2 is also detected in SVZ progenitors and *Tbr1* in layer VI neurons. For WT and double KO embryos, high magnification views of the cortex (a',d', m', q') and olfactory bulbs (a", d", l', p', u') are shown. For the double KO brains, two sections are shown (i,j,m,n), taken at the levels indicated in the diagram. Note in the *Dmrt3+/-;Dmrt5-/-* and double KO embryos the presence of a prominent olfactory bulb-like structure occupying most of the reduced cortex (shown schematically in the diagram in comparison to controls) in which *Tbr1*, Tbr2 and *Tbx21* are expressed and form a cluster or appear as a disorganized layer (l', p', u'). Note also in the cortex the disappearance of cortical Tbr2+ basal progenitors (compare a' and m') and more diffuse *Tbr1* expression (compare d' and q'). An asterisk indicates a region of strong ectopic expression of *Tbr2* outside the cortex in the double KO embryos. Abbreviation: AOB, accessory olfactory bulb; AON, anterior olfactory nucleus; BP, basal progenitor; Ctx, cortex, OB-L, olfactory bulb like structure; H, hippocampus; MCL, mitral cell layer; VI, layer VI cortical neurons. Scale bars: 50 µm.

Fig. 2. Genome-wide transcriptome analysis reveals that DMRT3 and DMRT5 cooperate to regulate cortical gene expression and play a role in early telencephalon dorsoventral patterning. (A) Dissected dorsal telencephalic tissues analyzed by RNA-seq and Venn diagram showing the overlap of differentially expressed genes (both up- and down-regulated) identified in *Dmrt3* KO, *Dmrt5* KO and double KO E12.5 embryos. (B) Heatmap for the 50 most significantly regulated genes (according to pvalue) in a comparison between wild type (WT) and double knockouts. Yellow and blue colors represent up- and downregulated genes, respectively. (C) Examples of identified differentially expressed dorsal and ventral genes with log2 fold changes observed in each genotype.

Fig. 3. Downregulation of dorsal determinants and expansion of dLGE markers in the lateral telencephalic neuroepithelium of *Dmrt3;Dmrt5* double KO embryos. (A, B) Coronal brain sections of E12.5 embryos hybridized with the indicated markers, with arrowheads indicating the region of the PSB and arrows pointing to the shifted dorsal limit of ventral markers expressed ectopically in the pallium of the double KO embryos. The strongly downregulated expression of *Emx1*, *Emx2* and *Ngn2* that remains detectable only in the dorsomedial telencephalon and the absence of *Dbx1* in the double KO is indicated by open arrows. The inset in the *Isl1* panel of the *Dmrt* double KO shows a high magnification view of the boxed region where some *Isl1* ectopic staining in the pallium is observed. (C) Diagram showing the expression domain of the different markers used in the telencephalon of E12.5 WT embryos and the reduction of the ventral pallium and an expansion of the dLGE domain as observed in *Dmrt3-/-;Dmrt5-/-*. Scale bar: 200 µm.

Fig. 4. Subpallial gene expression expands in the rostral telencephalon of *Dmrt3;Dmrt5* double KO embryos. Sagittal sections of E12.5 brains processed by ISH or IF with the indicated markers, with the rostral part to the right. Arrowheads indicate PSB. Arrows indicate the rostral or caudal boundaries of the gene expression domains. These boundaries are shifted dorsally in the *Dmrt3;Dmrt5* double KO embryos. Note in the mantle zone of the neuroepithelium of the single and double KO embryos *Pax6* staining in postmitotic cells that extends more caudally than in single KO or WT controls (open arrows). Scale bar: 200 µm.

Fig. 5. Dorsal telencephalon cells express ventral markers in *Dmrt3;Dmrt5* double KO embryos. (A) Coronal section of though E12.5 brains of the indicated genotypes processed by IF for Pax6 and Gsx2. High magnification views of the PSB are shown at the bottom. (B) Histograms showing the number of double positive cells among Pax6 positive cells in the boxed area (***P < 0.001).

Fig. 6. Expression of GABAergic, glutamatergic and olfactory bulb interneuron markers in the cortex of E18.5 Dmrt3 and Dmrt5 single KO and in double KO embryos. (A,O) Sagittal sections through brains of the indicated genotypes processed by ISH or IF for the indicated markers. In P, the line in the schematic of the brain of WT and double KO embryos indicate the positions of the sections. For the double KO brains, two sections are shown for each marker and a high magnification of the *Math2* and *Gad67* staining in the residual cortex of the double KO is shown in E',J'. Note the slight upregulation of *Gad67* (asterisks) and loss of *Math2* in the cortex of double KO embryos. Note also the TH positive cells that are not correctly laminated and form a large cluster in the olfactory bulb like structures of the double KO that extend more caudally in the dorsal telencephalon than in WT embryos (arrowheads). Ctx, cortex; OB, olfactory bulb; OB-L, olfactory bulb like structure, MFB, medial forebrain bundle, Acbn, accumbens nucleus. Scale bar: 500 µm except in H,P (50 µm).

Fig. 7. Repression of ventral and expansion of dorsal telencephalic and ventral pallium markers in the subpallium of *Dmrt5Tg/+;Foxg1-IRES-Cre* embryos. (A,B) Coronal sections through the telencephalon of transgenic and control embryos at E12.5 (A) and E13.5 (B) processed by ISH for the indicated markers. In A (upper 8 panels) arrowheads indicate the boundary of the MGE and LGE, a constant landmark between control and mutant mice, used for quantification of *Emx1* expansion (see text). Arrows point to the ventral limit of *Emx1* and *Ngn2* expression, or the dorsal limit of *Gsx2* and *Dlx2* expression. Notably in *Foxg1-IRES-Cre* embryos, the arrows and arrowheads are closer together than in controls, indicating the dorsalization of the telencephalon when *Dmrt5* is overexpressed. In A (lower 6 panels) and in B, arrrowheads indicate the PSB, and arrows indicate expression of *sFPR2*, *TGF-α*, *Sp8* and

Dbx1. (C) Diagram showing the ventral expansion of DP and VP markers as observed in the telencephalon of *Dmrt5Tg/Tg;Foxg1-IRES-Cre* embryos. (D) Dorsal view of P6 brains and eosin staining of olfactory bulbs. Arrowheads point to the RMS and the OV is indicated by an arrow. RMS, rostral migrating stream; OV, olfactory ventricule; GL, glomerular layer; Igr, internal granule layer.

Fig. 8. Repression of ventral and expansion of dorsal and ventral pallium markers in the subpallium of *Dmrt5Tg/Tg;Gsx2-Cre* embryos. (A,B) Coronal sections through the telencephalon of E12.5 embryos processed by IF (A) or ISH (B) with the indicated markers. In A, the ectopic expression of *Dmrt5* and downregulation of *Ascl1* and *Gsx2* in the ventral telencephalon are indicated by asterisks. In B, arrowheads indicate the region of the PSB. Arrows points to the expansion and shifted ventral limit of *Ngn2, Emx1* and *Dbx1* and downregulation and shifted dorsal limit of *Dlx2* expression in the subpallium of the transgenics. (C) Diagram showing the expansion of the ventral pallium as observed in *Dmrt5Tg/Tg;Gsx2-CIE* embryos. Scale bar: 200 um.

Fig. 9. DMRT5 and EMX2 cooperate in telencephalon D/V patterning. (A) Dorsal views of the head of E12.5 embryos. Hematoxylin and eosin staining of E12.5 brain coronal sections of the telencephalon, at rostral and caudal levels. The arrow points to the caudomedial cortex of the *Dmrt5;Emx2* double mutants, more severely reduced than in single mutants. **(B)** Coronal brain sections of E12.5 embryos processed by *in situ* hybridization with the indicated markers. Arrowheads indicate the region of the PSB. Arrows point to the dorsal limit of *Gsx2*, *Dlx2*, and *Ascl1* expression, shifted dorsally in the *Dmrt5- /-;Emx2-/-*. double KO embryos. The dramatic reduction of *Ngn2* in the cortex of the double KO embryos is indicated by an asterisk. Scale bar: 200 µm.

Fig. 10. DMRT5 forms a boundary with GSX2 at the PSB and the overexpression of *Gsx2* represses *Dmrt5* expression. (A) Coronal sections of the head of E14.5 *Gsx2GFP/+* knock-in embryos processed by IF with DMRT5 and GFP antibodies showing that at the PSB, cells expressing DMRT5 do not express GFP, that is, GSX2. The boxed area is shown at a high magnification on the left. Oe: olfactory epithelium. Scale bar: 200 µm. (B-E) Coronal sections through the telencephalon of E12.5 WT or *Foxg1tTA/+; tet-O-Gsx2-IRES-EGFP* double transgenic embryos immunostained with the indicated antibodies. In these transgenic embryos, *Gsx2* is misexpressed throughout the embryonic telencephalon and *Dmrt5* is reduced. Arrows in B, E points to the ventral limit of high *Dmrt5* expression.

Fig. 11. DMRT5 and EMX2 binds a Gsx2 ventral specific telencephalon enhancer. (A) UCSC genome browser view of the *Gsx2* locus with the location of the two cloned fragments tested in transgenic embryos. The identified putative DMRT3/5 and EMX2 binding sites are shown. (B) A lateral view and a coronal section of the head of a E12.5 *Gsx2* 1.8 kb enhancer LacZ reporter transgenic embryo (construct A) is shown on the left (scale bar: 500 µm for the lateral view and 200 µm for the coronal section). The level of the section is indicated by a dashed line. A coronal section of the brain of a Gsx2 1.3 kb enhancer-GFP reporter transgenic embryo (construct B) processed by DAB immunostaining for GFP and a high magnification view of the LGE region processed by IF for both GSX2 (red) and GFP (green) is shown on the right. (C) EMSA showing *in vitro* binding of cellular extracts containing DMRT3, DMRT5 and EMX2 or control extracts to BS3 of the *Gsx2* enhancer. DMRT3/5 and EMX2 complex formation is competed by WT enhancer oligonucleotides but not by oligonucleotides containing mutations in the DMRT and EMX2 binding sites. An arrowhead indicates a non-specific band.

REFERENCES

Allen ZJ, 2nd, Waclaw RR, Colbert MC, Campbell K (2007) Molecular identity of olfactory bulb interneurons: transcriptional codes of periglomerular neuron subtypes. J Mol Histol 38:517-525.

Anderson SA, Eisenstat DD, Shi L, Rubenstein JL (1997) Interneuron migration from basal forebrain to neocortex: dependence on Dlx genes. Science 278:474-476.

Aoto K, Nishimura T, Eto K, Motoyama J (2002) Mouse GLI3 regulates Fgf8 expression and apoptosis in the developing neural tube, face, and limb bud. Dev Biol 251:320-332.

Assimacopoulos S, Grove EA, Ragsdale CW (2003) Identification of a Pax6-dependent epidermal growth factor family signaling source at the lateral edge of the embryonic cerebral cortex. J Neurosci 23:6399-6403.

Backman M, Machon O, Mygland L, van den Bout CJ, Zhong W, Taketo MM, Krauss S (2005) Effects of canonical Wnt signaling on dorso-ventral specification of the mouse telencephalon. Dev Biol 279:155-168.

Bejerano G, Pheasant M, Makunin I, Stephen S, Kent WJ, Mattick JS, Haussler D (2004) Ultraconserved elements in the human genome. Science 304:1321-1325.

Berger MF, Badis G, Gehrke AR, Talukder S, Philippakis AA, Pena-Castillo L, Alleyne TM, Mnaimneh S, Botvinnik OB, Chan ET, Khalid F, Zhang W, Newburger D, Jaeger SA, Morris QD, Bulyk ML, Hughes TR (2008) Variation in homeodomain DNA binding revealed by high-resolution analysis of sequence preferences. Cell 133:1266-1276.

Besse L, Neti M, Anselme I, Gerhardt C, Ruther U, Laclef C, Schneider-Maunoury S (2011) Primary cilia control telencephalic patterning and morphogenesis via Gli3 proteolytic processing. Development 138:2079-2088.

Carney RS, Cocas LA, Hirata T, Mansfield K, Corbin JG (2009) Differential regulation of telencephalic pallial-subpallial boundary patterning by Pax6 and Gsh2. Cereb Cortex 19:745-759.

Chiang C, Litingtung Y, Lee E, Young KE, Corden JL, Westphal H, Beachy PA (1996) Cyclopia and defective axial patterning in mice lacking Sonic hedgehog gene function. Nature 383:407-413.

Chotteau-Lelievre A, Desbiens X, Pelczar H, Defossez PA, de Launoit Y (1997) Differential expression patterns of the PEA3 group transcription factors through murine embryonic development. Oncogene 15:937-952.

Corbin JG, Gaiano N, Machold RP, Langston A, Fishell G (2000) The Gsh2 homeodomain gene controls multiple aspects of telencephalic development. Development 127:5007-5020.

De Clercq S, Keruzore M, Desmaris E, Pollart C, Assimacopoulos S, Preillon J, Ascenzo S, Matson CK, Lee M, Nan X, Li M, Nakagawa Y, Hochepied T, Zarkower D, Grove EA, Bellefroid EJ (2018) DMRT5 Together with DMRT3 Directly Controls Hippocampus Development and Neocortical Area Map Formation. Cereb Cortex 28:493-509.

Ehrman LA, Mu X, Waclaw RR, Yoshida Y, Vorhees CV, Klein WH, Campbell K (2013) The LIM homeobox gene Isl1 is required for the correct development of the striatonigral pathway in the mouse. Proc Natl Acad Sci U S A 110:E4026-4035.

Ericson J, Muhr J, Placzek M, Lints T, Jessell TM, Edlund T (1995) Sonic hedgehog induces the differentiation of ventral forebrain neurons: a common signal for ventral patterning within the neural tube. Cell 81:747-756.

Faedo A, Ficara F, Ghiani M, Aiuti A, Rubenstein JL, Bulfone A (2002) Developmental expression of the T-box transcription factor T-bet/Tbx21 during mouse embryogenesis. Mech Dev 116:157-160.

Fernandes M, Gutin G, Alcorn H, McConnell SK, Hebert JM (2007) Mutations in the BMP pathway in mice support the existence of two molecular classes of holoprosencephaly. Development 134:3789-3794.

Flames N, Pla R, Gelman DM, Rubenstein JL, Puelles L, Marin O (2007) Delineation of multiple subpallial progenitor domains by the combinatorial expression of transcriptional codes. J Neurosci 27:9682-9695.

Fode C, Ma Q, Casarosa S, Ang SL, Anderson DJ, Guillemot F (2000) A role for neural determination genes in specifying the dorsoventral identity of telencephalic neurons. Genes Dev 14:67-80.

Gaitanis JN, Walsh CA (2004) Genetics of disorders of cortical development. Neuroimaging Clin N Am 14:219-229, viii.

Grove EA, Tole S, Limon J, Yip L, Ragsdale CW (1998) The hem of the embryonic cerebral cortex is defined by the expression of multiple Wnt genes and is compromised in Gli3-deficient mice. Development 125:2315-2325.

Gutin G, Fernandes M, Palazzolo L, Paek H, Yu K, Ornitz DM, McConnell SK, Hebert JM (2006) FGF signalling generates ventral telencephalic cells independently of SHH. Development 133:2937-2946.

Hasenpusch-Theil K, Watson JA, Theil T (2017) Direct Interactions Between Gli3, Wnt8b, and Fgfs Underlie Patterning of the Dorsal Telencephalon. Cereb Cortex 27:1137-1148.

Hasenpusch-Theil K, Magnani D, Amaniti EM, Han L, Armstrong D, Theil T (2012) Transcriptional analysis of Gli3 mutants identifies Wnt target genes in the developing hippocampus. Cereb Cortex 22:2878-2893.

Hu WF, Chahrour MH, Walsh CA (2014) The diverse genetic landscape of neurodevelopmental disorders. Annu Rev Genomics Hum Genet 15:195-213.

Huber K, Narasimhan P, Shtukmaster S, Pfeifer D, Evans SM, Sun Y (2013) The LIM-Homeodomain transcription factor Islet-1 is required for the development of sympathetic neurons and adrenal chromaffin cells. Dev Biol 380:286-298.

Kahoud RJ, Elsen GE, Hevner RF, Hodge RD (2014) Conditional ablation of Tbr2 results in abnormal development of the olfactory bulbs and subventricular zone-rostral migratory stream. Dev Dyn 243:440-450.

Kawaguchi D, Sahara S, Zembrzycki A, O'Leary DDM (2016) Generation and analysis of an improved Foxg1-IRES-Cre driver mouse line. Dev Biol 412:139-147.

Konno D, Iwashita M, Satoh Y, Momiyama A, Abe T, Kiyonari H, Matsuzaki F (2012) The mammalian DM domain transcription factor Dmrta2 is required for early embryonic development of the cerebral cortex. PLoS One 7:e46577.

Kroll TT, O'Leary DD (2005) Ventralized dorsal telencephalic progenitors in Pax6 mutant mice generate GABA interneurons of a lateral ganglionic eminence fate. Proc Natl Acad Sci U S A 102:7374-7379.

Kuschel S, Ruther U, Theil T (2003) A disrupted balance between Bmp/Wnt and Fgf signaling underlies the ventralization of the Gli3 mutant telencephalon. Dev Biol 260:484-495.

Murphy MW, Zarkower D, Bardwell VJ (2007) Vertebrate DM domain proteins bind similar DNA sequences and can heterodimerize on DNA. BMC Mol Biol 8:58.

Muzio L, Di Benedetto B, Stoykova A, Boncinelli E, Gruss P, Mallamaci A (2002a) Emx2 and Pax6 control regionalization of the pre-neuronogenic cortical primordium. Cereb Cortex 12:129-139.

Muzio L, Di Benedetto B, Stoykova A, Boncinelli E, Gruss P, Mallamaci A (2002b) Conversion of cerebral cortex into basal ganglia in Emx2(-/-) Pax6(Sey/Sey) double-mutant mice. Nat Neurosci 5:737-745.

Ohkubo Y, Chiang C, Rubenstein JL (2002) Coordinate regulation and synergistic actions of BMP4, SHH and FGF8 in the rostral prosencephalon regulate morphogenesis of the telencephalic and optic vesicles. Neuroscience 111:1-17.

Pellegrini M, Mansouri A, Simeone A, Boncinelli E, Gruss P (1996) Dentate gyrus formation requires Emx2. Development 122:3893-3898.

Pennacchio LA, Ahituv N, Moses AM, Prabhakar S, Nobrega MA, Shoukry M, Minovitsky S, Dubchak I, Holt A, Lewis KD, Plajzer-Frick I, Akiyama J, De Val S, Afzal V, Black BL, Couronne O, Eisen MB, Visel A, Rubin EM (2006) In vivo enhancer analysis of human conserved non-coding sequences. Nature 444:499-502.

Porteus MH, Bulfone A, Ciaranello RD, Rubenstein JL (1991) Isolation and characterization of a novel cDNA clone encoding a homeodomain that is developmentally regulated in the ventral forebrain. Neuron 7:221-229.

Puelles L, Kuwana E, Puelles E, Bulfone A, Shimamura K, Keleher J, Smiga S, Rubenstein JL (2000) Pallial and subpallial derivatives in the embryonic chick and mouse telencephalon, traced by the expression of the genes Dlx-2, Emx-1, Nkx-2.1, Pax-6, and Tbr-1. J Comp Neurol 424:409-438.

Qin S, Madhavan M, Waclaw RR, Nakafuku M, Campbell K (2016) Characterization of a new Gsx2-cre line in the developing mouse telencephalon. Genesis 54:542-549.

Rallu M, Machold R, Gaiano N, Corbin JG, McMahon AP, Fishell G (2002) Dorsoventral patterning is established in the telencephalon of mutants lacking both Gli3 and Hedgehog signaling. Development 129:4963-4974.

Rash BG, Grove EA (2007) Patterning the dorsal telencephalon: a role for sonic hedgehog? J Neurosci 27:11595-11603.

Sahara S, Kawakami Y, Izpisua Belmonte JC, O'Leary DD (2007) Sp8 exhibits reciprocal induction with Fgf8 but has an opposing effect on anterior-posterior cortical area patterning. Neural Dev 2:10.

Saulnier A, Keruzore M, De Clercq S, Bar I, Moers V, Magnani D, Walcher T, Filippis C, Kricha S, Parlier D, Viviani L, Matson CK, Nakagawa Y, Theil T, Gotz M, Mallamaci A, Marine JC, Zarkower D, Bellefroid EJ (2013) The doublesex homolog Dmrt5 is required for the development of the caudomedial cerebral cortex in mammals. Cereb Cortex 23:2552-2567.

Shimogori T, Banuchi V, Ng HY, Strauss JB, Grove EA (2004) Embryonic signaling centers expressing BMP, WNT and FGF proteins interact to pattern the cerebral cortex. Development 131:5639-5647.

Stenman J, Toresson H, Campbell K (2003) Identification of two distinct progenitor populations in the lateral ganglionic eminence: implications for striatal and olfactory bulb neurogenesis. J Neurosci 23:167-174.

Storm EE, Garel S, Borello U, Hebert JM, Martinez S, McConnell SK, Martin GR, Rubenstein JL (2006) Dose-dependent functions of Fgf8 in regulating telencephalic patterning centers. Development 133:1831-1844.

Stoykova A, Treichel D, Hallonet M, Gruss P (2000) Pax6 modulates the dorsoventral patterning of the mammalian telencephalon. J Neurosci 20:8042-8050.

Sun J, Rockowitz S, Xie Q, Ashery-Padan R, Zheng D, Cvekl A (2015) Identification of in vivo DNA-binding mechanisms of Pax6 and reconstruction of Pax6-dependent gene regulatory networks during forebrain and lens development. Nucleic Acids Res 43:6827-6846.

Theil T, Alvarez-Bolado G, Walter A, Ruther U (1999) Gli3 is required for Emx gene expression during dorsal telencephalon development. Development 126:3561-3571.

Tole S, Hébert J (2013) Chapter 1 – Telencephalon Patterning: Patterning and Cell Type Specification in the Developing CNS and PNS. Comprehensive Developmental Neuroscience: 3–24.

Tole S, Ragsdale CW, Grove EA (2000a) Dorsoventral patterning of the telencephalon is disrupted in the mouse mutant extra-toes(J). Dev Biol 217:254-265.

Tole S, Goudreau G, Assimacopoulos S, Grove EA (2000b) Emx2 is required for growth of the hippocampus but not for hippocampal field specification. J Neurosci 20:2618-2625.

Tole S, Remedios R, Saha B, Stoykova A (2005) Selective requirement of Pax6, but not Emx2, in the specification and development of several nuclei of the amygdaloid complex. J Neurosci 25:2753-2760.

Toresson H, Campbell K (2001) A role for Gsh1 in the developing striatum and olfactory bulb of Gsh2 mutant mice. Development 128:4769-4780.

Toresson H, Potter SS, Campbell K (2000) Genetic control of dorsal-ventral identity in the telencephalon: opposing roles for Pax6 and Gsh2. Development 127:4361-4371.

Urquhart JE, Beaman G, Byers H, Roberts NA, Chervinsky E, O'Sullivan J, Pilz D, Fry A, Williams SG, Bhaskar SS, Khayat M, Simanovsky N, Shachar IB, Shalev SA, Newman WG (2016) DMRTA2 (DMRT5) is mutated in a novel cortical brain malformation. Clin Genet 89:724-727.

Waclaw RR, Ehrman LA, Pierani A, Campbell K (2010) Developmental origin of the neuronal subtypes that comprise the amygdalar fear circuit in the mouse. J Neurosci 30:6944-6953.

Waclaw RR, Wang B, Pei Z, Ehrman LA, Campbell K (2009) Distinct temporal requirements for the homeobox gene Gsx2 in specifying striatal and olfactory bulb neuronal fates. Neuron 63:451-465.

Waclaw RR, Allen ZJ, 2nd, Bell SM, Erdelyi F, Szabo G, Potter SS, Campbell K (2006) The zinc finger transcription factor Sp8 regulates the generation and diversity of olfactory bulb interneurons. Neuron 49:503-516.

Wang B, Waclaw RR, Allen ZJ, 2nd, Guillemot F, Campbell K (2009) Ascl1 is a required downstream effector of Gsx gene function in the embryonic mouse telencephalon. Neural Dev 4:5.

Wang B, Long JE, Flandin P, Pla R, Waclaw RR, Campbell K, Rubenstein JL (2013) Loss of Gsx1 and Gsx2 function rescues distinct phenotypes in Dlx1/2 mutants. J Comp Neurol 521:1561-1584.

Yee SP, Rigby PW (1993) The regulation of myogenin gene expression during the embryonic development of the mouse. Genes Dev 7:1277-1289.

Yoshida M, Suda Y, Matsuo I, Miyamoto N, Takeda N, Kuratani S, Aizawa S (1997) Emx1 and Emx2 functions in development of dorsal telencephalon. Development 124:101-111.

Young FI, Keruzore M, Nan X, Gennet N, Bellefroid EJ, Li M (2017) The doublesex-related

Yun K, Potter S, Rubenstein JL (2001) Gsh2 and Pax6 play complementary roles in dorsoventral patterning of the mammalian telencephalon. Development 128:193-205.

Yun K, Garel S, Fischman S, Rubenstein JL (2003) Patterning of the lateral ganglionic eminence by the Gsh1 and Gsh2 homeobox genes regulates striatal and olfactory bulb histogenesis and the growth of axons through the basal ganglia. J Comp Neurol 461:151-165.

Figure 1

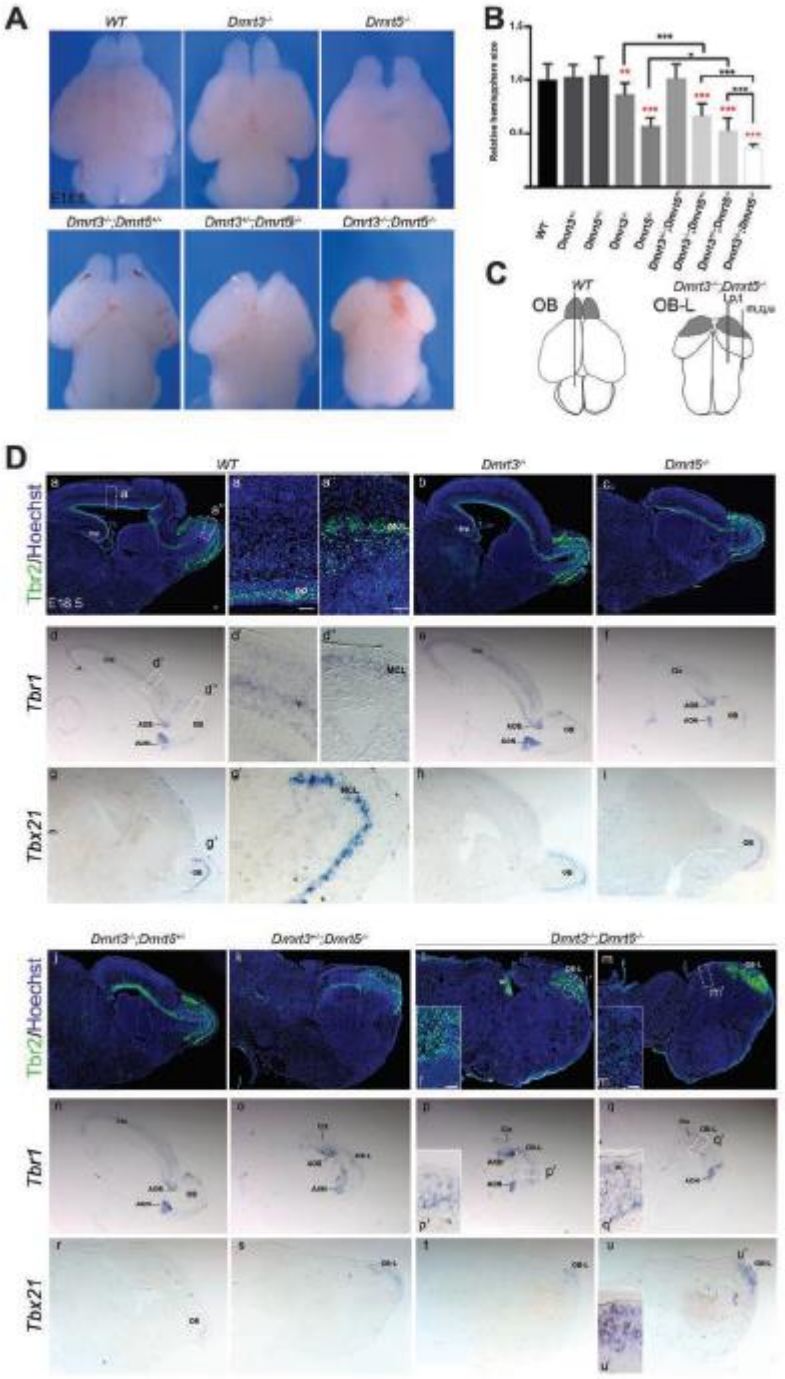
A
WT
Dmrt3-/-
Dmrt5-/-
Dmrt3+/-;Dmrt5+/-
Dmrt3+/-;Dmrt5-/-
Dmrt3-/-;Dmrt5-/-
B
C
WT
OB
Dmrt3-/-;Dmrt5-/-
OB-L
D
WT
Dmrt3-/-
Dmrt5-/-
Tbr2/Hoechst
Tbr1
Tbx21
Dmrt3+/-;Dmrt5+/-
Dmrt3+/-;Dmrt5-/-
Dmrt3-/-;Dmrt5-/-

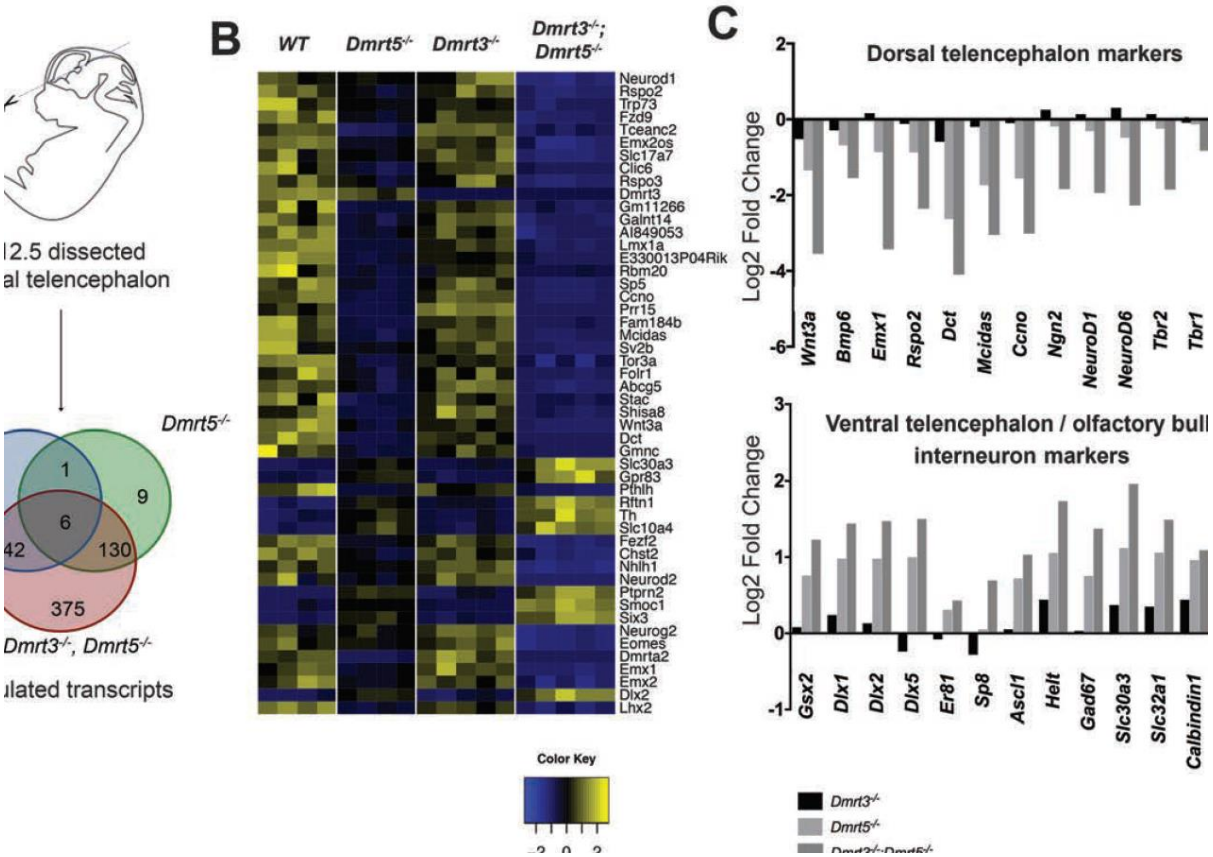
12.5 dissected
al telencephalon
Dmrt5-/-
1
9
6
42
130
375
Dmrt3-/-, Dmrt5-/-
ulated transcripts
B
WT
Dmrt5-/-
Dmrt3-/-
Dmrt3-/-; Dmrt5-/-
Neurod1
Rspo2
Trp73
Fzd9
Tceanc2
Emx2os
Slc17a7
Clic6
Rspo3
Dmrt3
Gm11266
Galnt14
AI849053
Lmx1a
E330013P04Rik
Rbm20
Sp5
Ccno
Prr15
Fam184b
Mcidas
Sv2b
Tor3a
Folr1
Abcg5
Stac
Shisa8
Wnt3a
Dct
Gmnc
Slc30a3
Gpr83
Pthlh
Rftn1
Th
Slc10a4
Fezf2
Chst2
Nhlh1
Neurod2
Ptprn2
Srhoc1
Six3
Neurog2
Eomes
Dmrta2
Emx1
Emx2
Dlx2
Lhx2
Color Key
C
Dorsal telencephalon markers
Log2 Fold Change
2
0
-2
-4
-6
Wnt3a
Bmp6
Emx1
Rspo2
Dct
Mcidas
Ccno
Ngn2
NeuroD1
NeuroD6
Tbr2
Tbr1
Ventral telencephalon / olfactory bul
interneuron markers
Log2 Fold Change
3
2
1
0
-1
Gsx2
Dlx1
Dlx2
Dlx5
Er81
Sp8
Ascl1
Helt
Gad67
Slc30a3
Slc32a1
Calbindin1
Dmrt3-/-
Dmrt5-/-

Figure 3

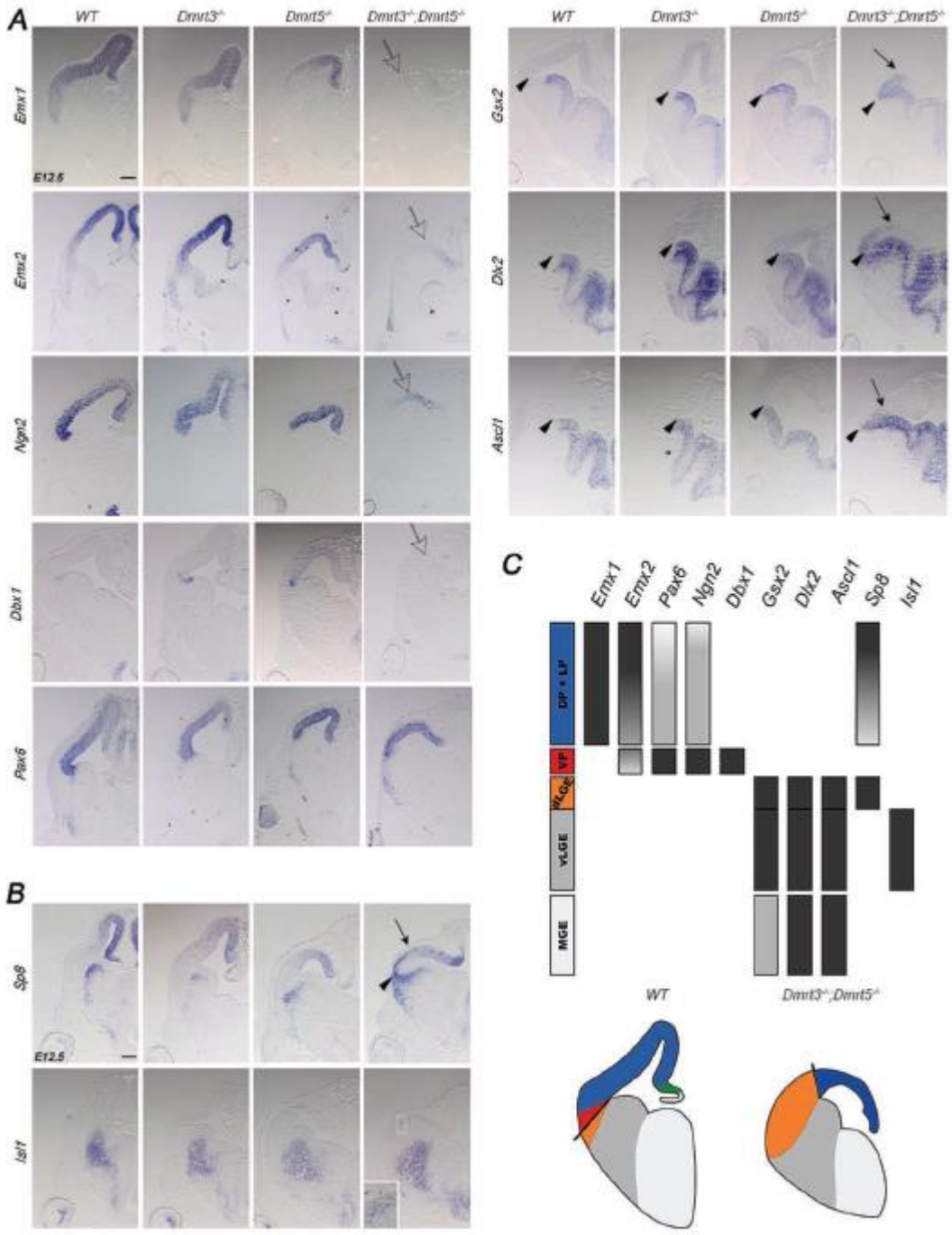
A
WT
Dmrt3-/-
Dmrt5-/-
Dmrt3-/-;Dmrt5-/-
Emx1
E12.5
Emx2
Ngn2
Dbx1
Pax6
Gsx2
Dlx2
Ascl1
B
Sp8
Isl1
C
Emx1
Emx2
Pax6
Ngn2
Dbx1
Gsx2
Dlx2
Ascl1
Sp8
Isl1
DP + LP
VP
vLGE
MGE
WT
Dmrt3-/-;Dmrt5-/-

Figure 4

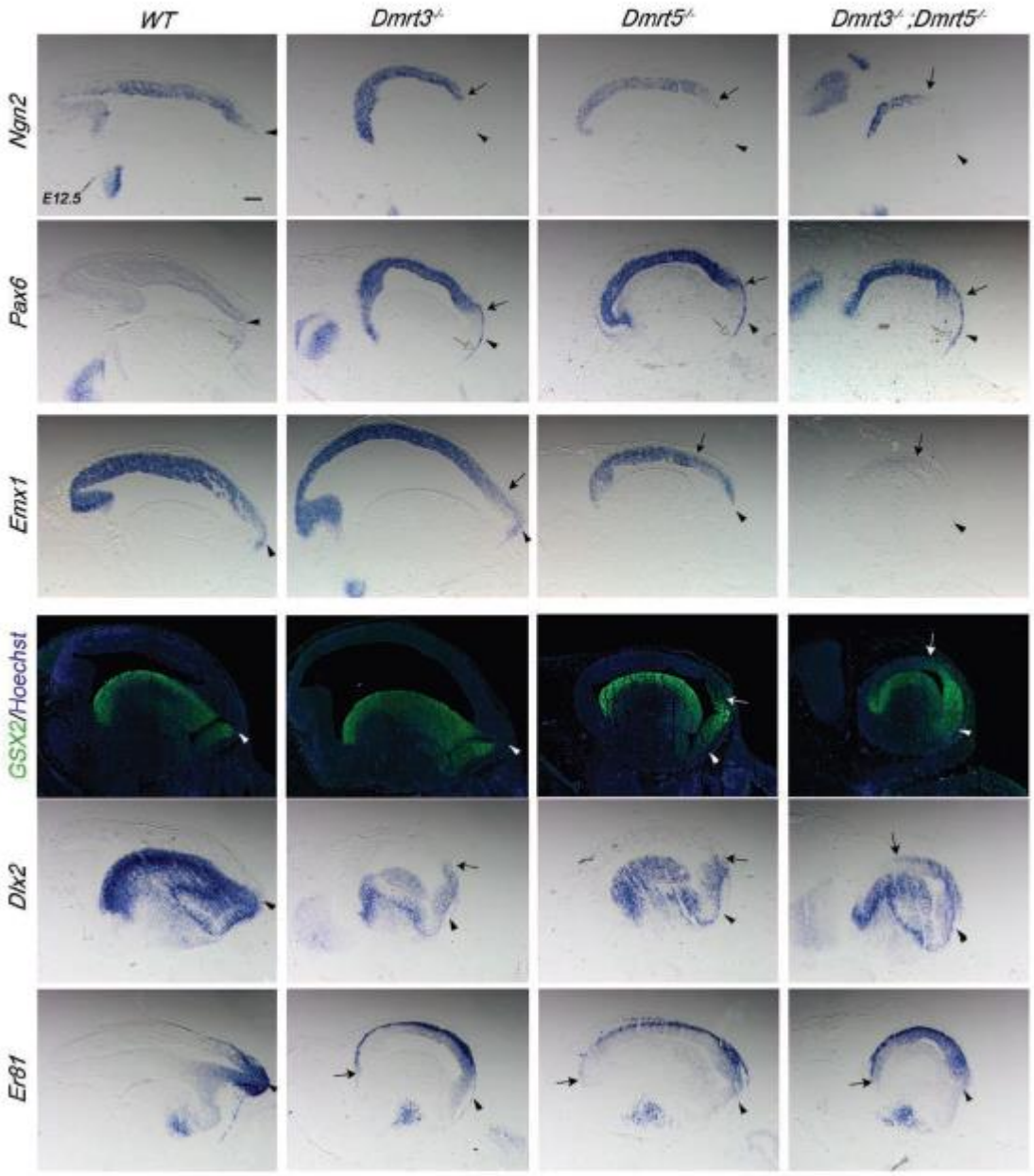
WT
Dmrt3-/-
Dmrt5-/-
Dmrt3-/-;Dmrt5-/-
Ngn2
E12.5
Pax6
Emx1
GSX2/Hoechst
Dlx2
Er81

Figure 5

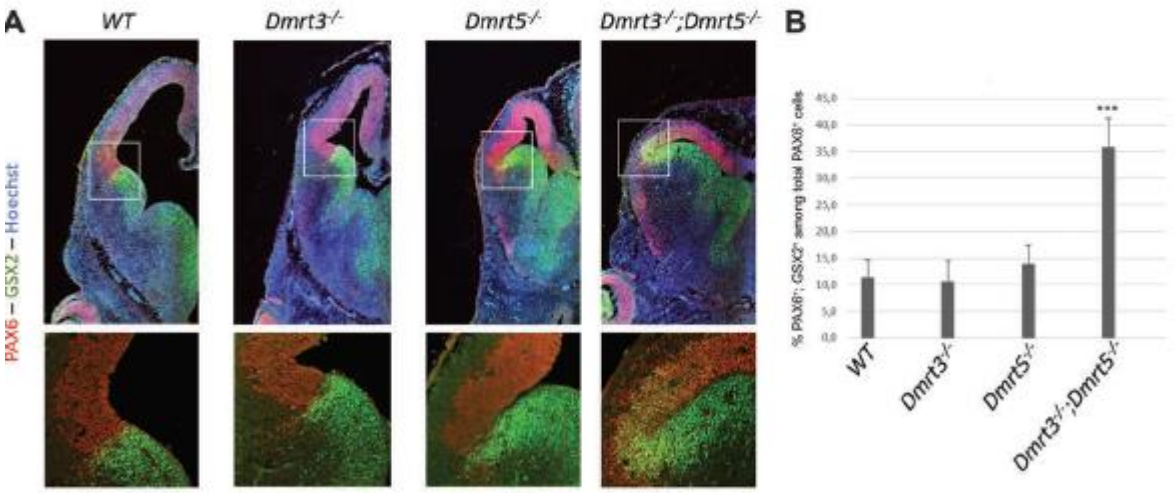

Figure 6

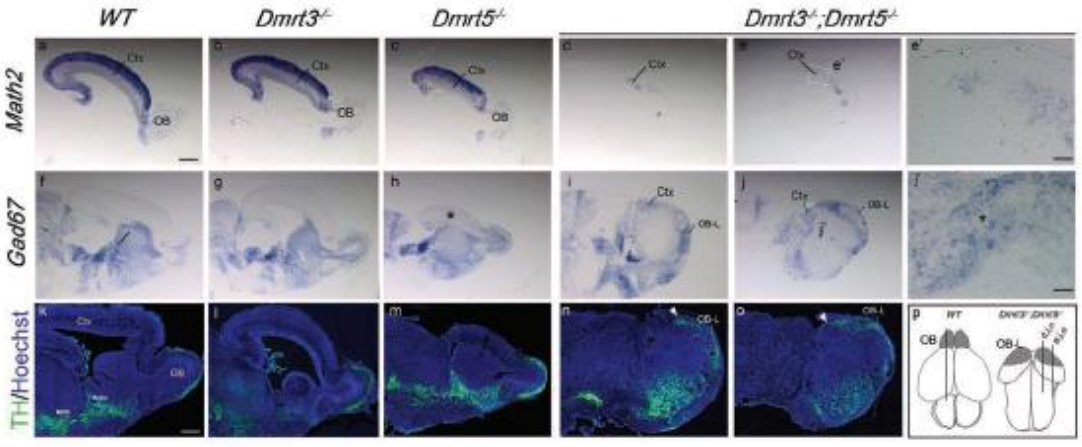

Figure 7

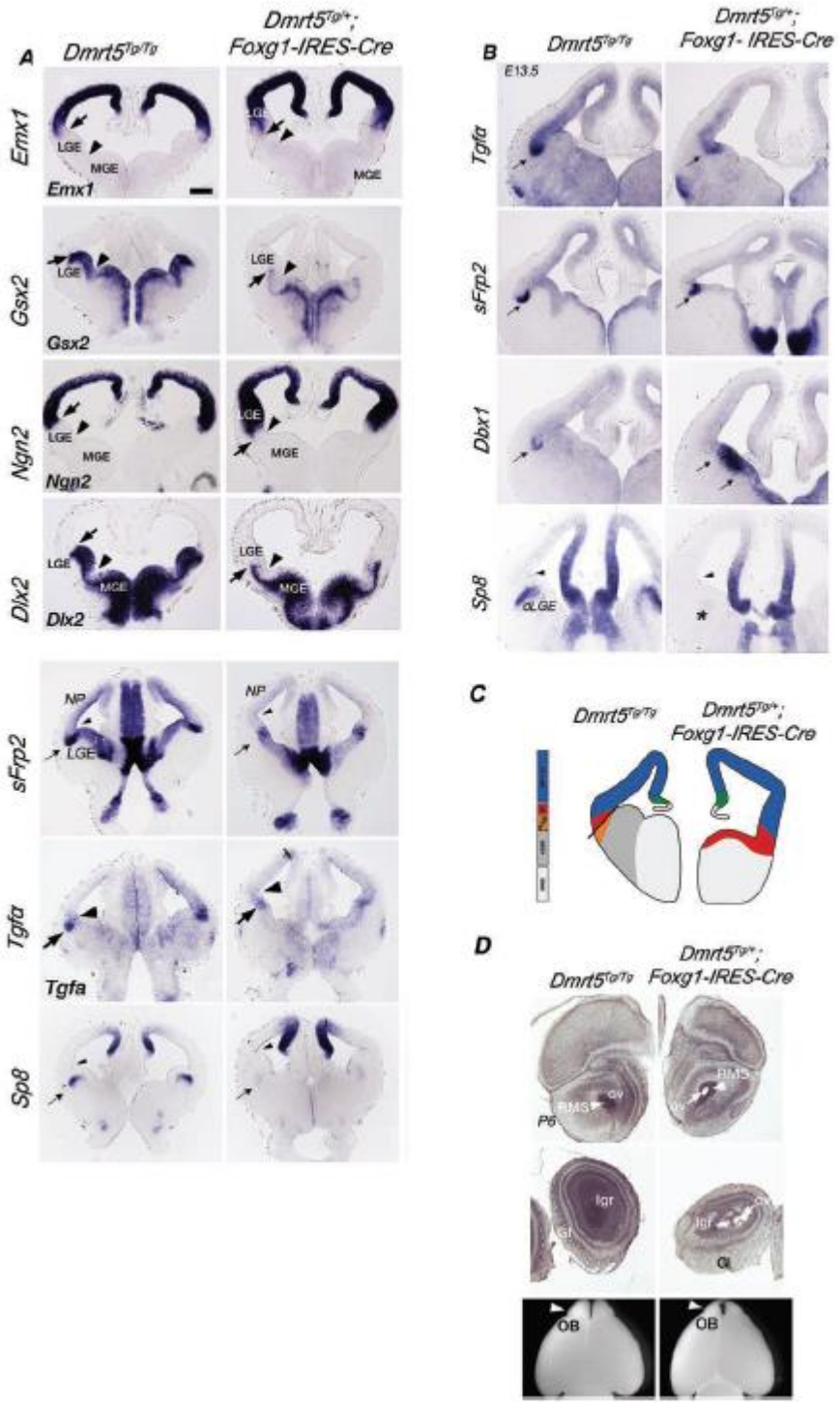
A
Dmrt5Tg/Tg
Dmrt5Tg/+; Foxg1-IRES-Cre
Emx1
Gsx2
Ngn2
Dlx2
sFrp2
Tgfa
Sp8
LGE
MGE
NP
B
Dmrt5Tg/Tg
Dmrt5Tg/+; Foxg1- IRES-Cre
E13.5
Tgfa
sFrp2
Dbx1
Sp8
aLGE
C
Dmrt5Tg/Tg
Dmrt5Tg/+; Foxg1-IRES-Cre
D
Dmrt5Tg/Tg
Dmrt5Tg/+; Foxg1-IRES-Cre
P6
RMS
OB

Figure 8

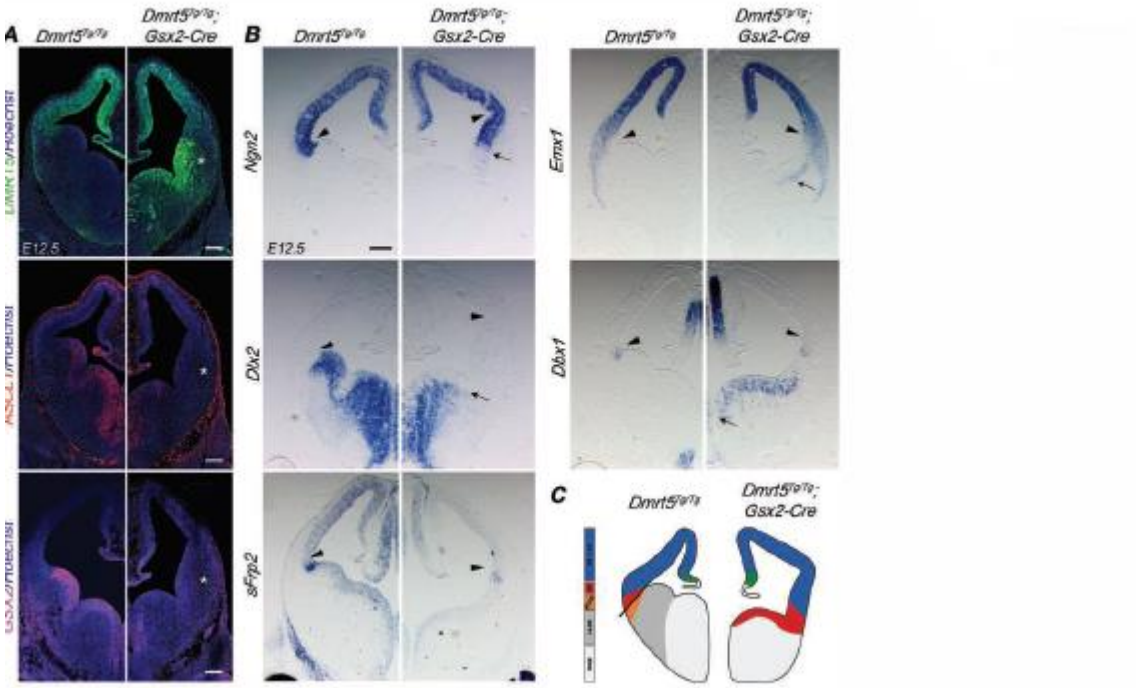
A
Dmrt5tg/tg
Dmrt5tg/tg; Gsx2-Cre
E12.5
B
Dmrt5tg/tg
Dmrt5tg/tg; Gsx2-Cre
Ngn2
Dlx2
sFrp2
E12.5
Dmrt5tg/tg
Dmrt5tg/tg; Gsx2-Cre
Emx1
Dbx1
C
Dmrt5tg/tg
Dmrt5tg/tg; Gsx2-Cre

Figure 9

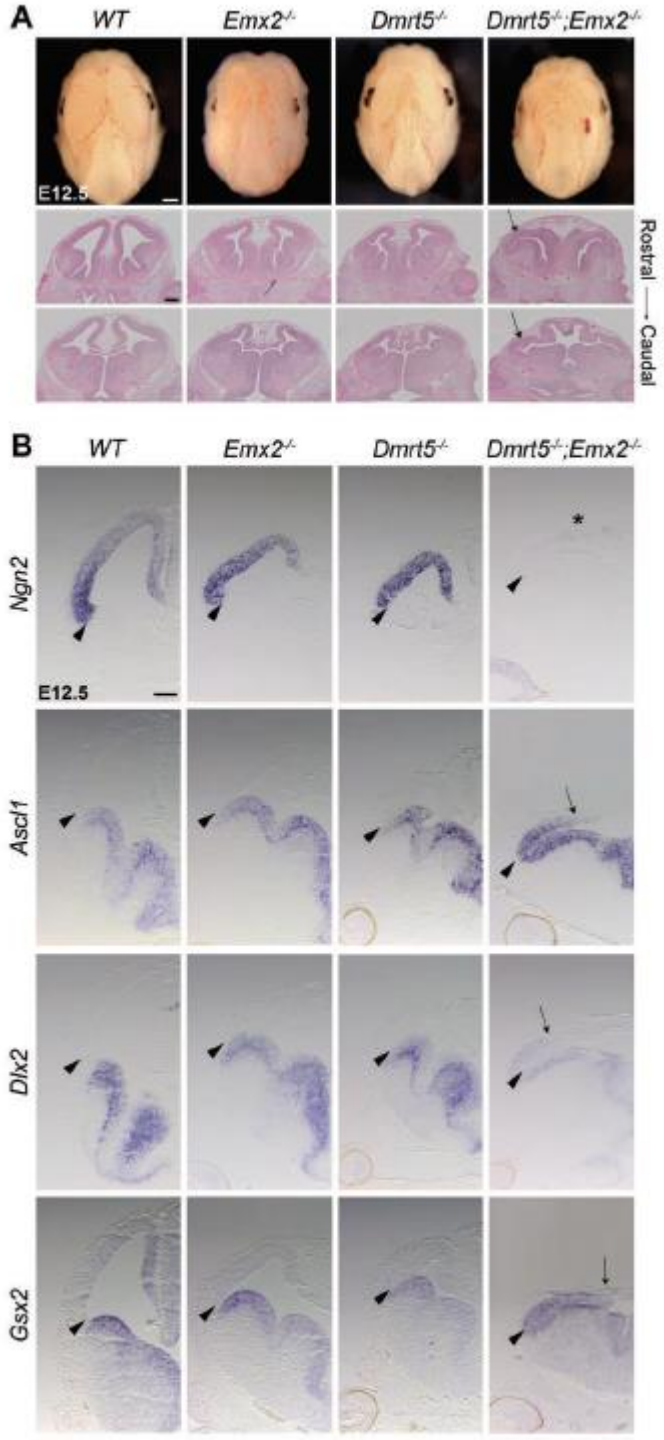
A
WT
Emx2-/-
Dmrt5-/-
Dmrt5-/-;Emx2-/-
E12.5
Rostral
Caudal
B
WT
Emx2-/-
Dmrt5-/-
Dmrt5-/-;Emx2-/-
Ngn2
E12.5
Ascl1
Dlx2
Gsx2

Figure 10

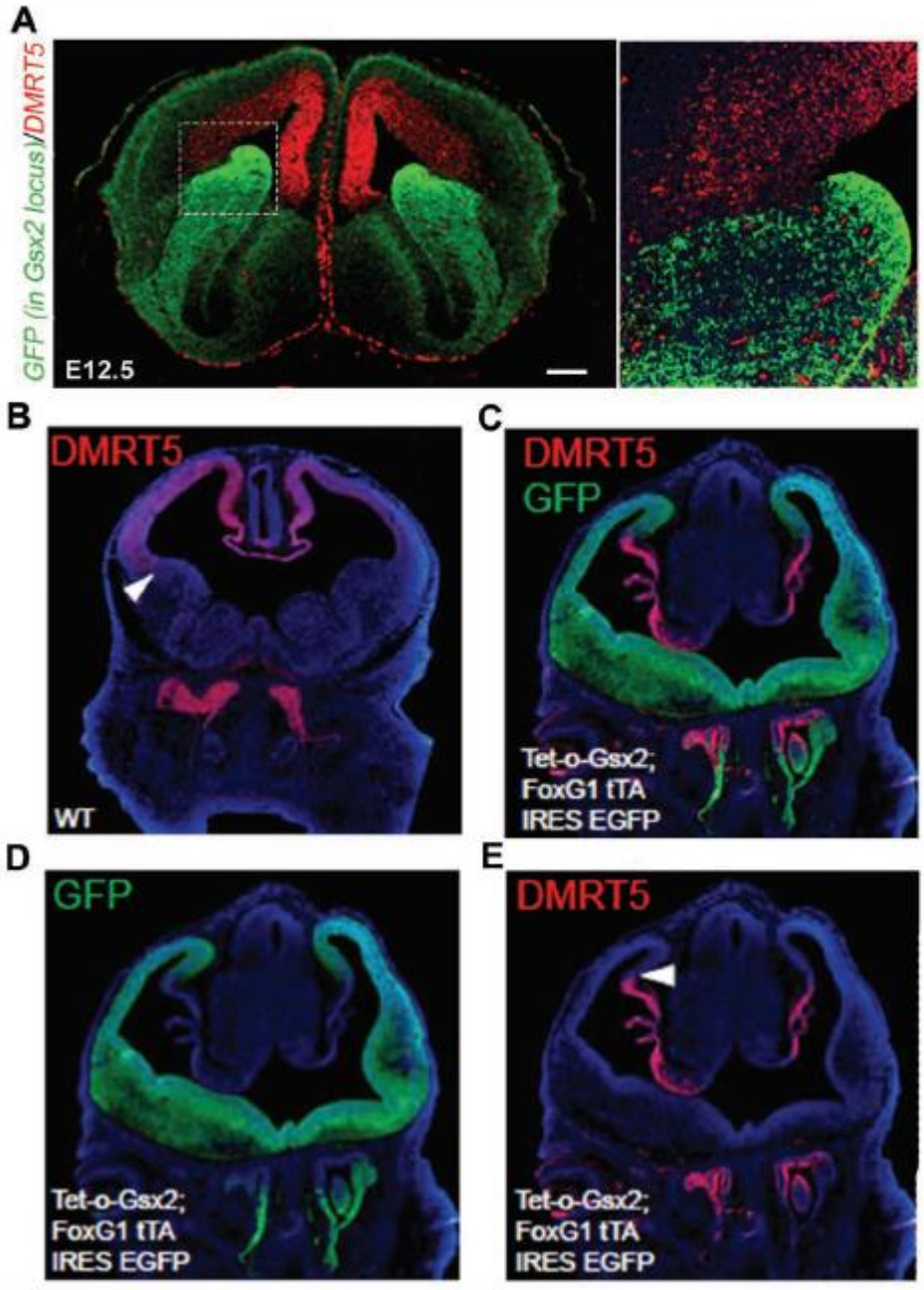
A
GFP (in Gsx2 locus)/DMRT5
E12.5
B
DMRT5
WT
C
DMRT5
GFP
Tet-o-Gsx2;
FoxG1 tTA
IRES EGFP
D
GFP
Tet-o-Gsx2;
FoxG1 tTA
IRES EGFP
E
DMRT5
Tet-o-Gsx2;
FoxG1 tTA
IRES EGFP

Figure 11

A

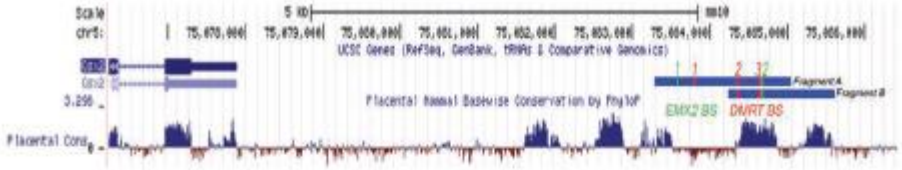

DMRT5 consensus sequence (Murphy et al. 2007)	
DMRT3 consensus sequence (Murphy et al. 2007)	
EMX2 consensus sequence (Berger et al. 2008)	
DMRT BS3/EMX2 BS2	GACTTTTCGATACATTCCTAATTGACTGAGGG
mDMRT BS3/mEMX2 BS2	GACTTTTCCATACATTCCTACGTGACTGAGGG

B

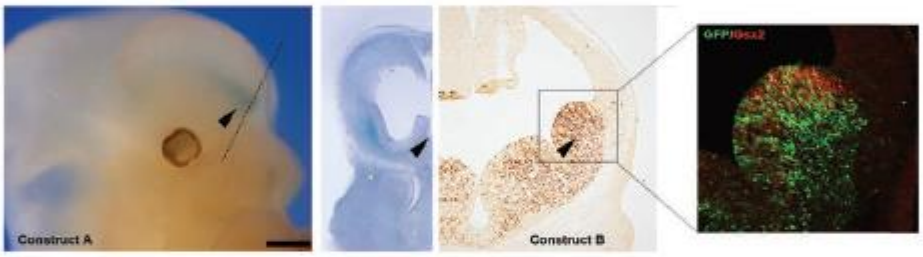

C

extracts \ probes	DMRT BS3/EMX2 BS2					
competitor	,	,	,	,	mDBS3/mE2	DBS3/E2
DMRT3	-	+	-	+	+	+
EMX2	-	-	+	+	+	+

extracts \ probes	DMRT BS3/EMX2 BS2					
competitor	,	,	,	,	mDBS3/mE2	DBS3/E2
DMRT5	-	+	-	+	+	+
EMX2	-	-	+	+	+	+